

Critical dynamics of gene networks is a mechanism behind ageing and Gompertz law

D. Podolskiy¹, I. Molodtsov^{2,3}, A. Zenin³, V. Kogan^{2,3}, L. I. Menshikov³, Robert J. Shmookler Reis^{4,5,6} & P. O. Fedichev^{2,3}

¹*Massachusetts Institute of Technology, 77 Massachusetts Ave., Cambridge, MA, 02139, USA*

²*Moscow Institute of Physics and Technology, 141700,*

Institutskii per. 9, Dolgoprudny, Moscow Region, Russian Federation,

³*Quantum Pharmaceuticals Ltd, Ul. Kosmonavta Volkova 6A-1205, 125171, Moscow, Russian Federation,*

⁴*McClellan VA Medical Center, Central Arkansas Veterans Healthcare System, Little Rock, AR, USA*

⁵*Department of Biochemistry and Molecular Biology,*

University of Arkansas for Medical Sciences, Little Rock, AR, USA and

⁶*Department of Geriatrics, University of Arkansas for Medical Sciences, Little Rock, AR, USA*

Although it has long been suggested that accumulation of errors in transcription and translation is one of the most important molecular mechanisms leading to ageing, a quantitative link between the error accumulation dynamics and mortality of species has so far remained elusive. We study stability properties of a generic gene regulatory network (GRN) and demonstrate that phenomenology of ageing and the associated population mortality rate can be naturally described in terms of critical dynamics of gene regulation and metabolic profiles. We analyze age-dependent microarray datasets and metabolic profiles for *Drosophila melanogaster* and explicitly show that the resulting GRNs are nearly critical and inherently unstable. This instability manifests itself as ageing in the form of exponential distortions of gene expressions and metabolic profiles with age, and causes the characteristic increase in mortality rate with age as described by the Gompertz law. On top of that we explain the plateau in mortality rates observed at very late ages for large populations. We show that ageing contains both a stochastic component, related to regulatory error accumulation in transcription/translation/metabolic pathways, and a strong deterministic component, which can be naturally associated with a part of a development programme. We conclude on this basis that two opposing hypotheses of ageing, error accumulation and programmed ageing are in fact compatible with each other. Since mortality in humans, where it is characterized best, is mostly associated with age related diseases, we support the idea of ageing being the driving force behind the development of major diseases.

INTRODUCTION

Ageing is a complicated interplay of different processes in a living matter. The processes influenced by and affecting ageing take place at every possible scale characterizing the living organism, ranging from a single cell level (*e.g.*, oxidative damage to cells, or somatic mutations) to the level of interaction between different body organs (*e.g.*, failure of individual organs with age or accumulation of dangerous byproducts of metabolic activity such as arterial plaque). This is why it has been notoriously difficult to pinpoint the ultimate cause, a single molecular mechanism behind ageing and relate it to such life-long consequences as progression of chronic age-related diseases and, ultimately, mortality. As a consequence, a wide spectrum of propositions on the origin of ageing has emerged over the years such as the hypothesis of damage accumulation [1–4], the hyperfunction theory [5, 6], the disposable soma hypothesis [7, 8] and antagonistic pleiotropy [9]. Since the theories of ageing, often very different from each other in both spirit and letter, reflect upon different “facets” of ageing [10], it is not always possible to see their mutual inconsistencies and compatibilities. In particular, there seems to exist a major collision between theories that view ageing as a pre-programmed process [5, 6, 11–13] or a stochastic process associated with damage/error accumulation [1–4]. We shall argue here that these two ideas are in fact fully compatible

with each other.

The argument is based on the hypothesis suggested nearly 40 years ago by Leslie Orgel [14] (see also [15, 16]), that one of the molecular-level processes responsible for ageing is the accumulation of translation and transcription errors in cells, exceeding the ability of cellular damage-response pathways to repair. Recently we have performed a semi-quantitative study of a generic GRN stability and suggested a causal relation between the accumulation of the regulatory errors, mortality increase and ageing [17]. However, the underlying mechanistic level details of the interplay between the dynamics of error accumulation in transcription/translation/metabolic processes and the increase in mortality rates has not yet been clearly established.

To identify such a link, we develop a theory of stochastic critical dynamics of GRN and show, that under very generic assumptions, GRNs of most species are inherently unstable. Applying the method of proper orthogonal decomposition common in “Big Data” analysis [18] to the publicly available age-variable transcriptome and metabolome datasets for *Drosophila melanogaster* [19, 20], we demonstrate explicitly, that the auto-correlation functions of transcriptional and metabolic datasets for *D. melanogaster* exhibit stochastic exponential instability with a characteristic time scale, t_α , which is of the same order as mortality rate doubling time t_{MRDT} of *D. melanogaster*. We provide explicit solutions for the

stochastic ageing dynamics of realistic GRNs, obtain expressions for age-dependent mortality increase. We argue that the two time scales, t_α and t_{MRDT} , should coincide for any other species subject to Gompertz mortality law. Therefore we are able to causally relate the GRN instability to the characteristic Gompertzian increase of mortality rate in populations. The exponential increase of mortality eventually slows down and the mortality rate is expected to approach a plateau, $M(t \gtrsim t_{\text{ls}}) \sim 1/t_{\text{MRDT}}$, at late ages, where t_{ls} is the mean lifespan of the species. The result should be valid for sufficiently long lived animals, $t_{\text{ls}} \gg t_\alpha$ and appears to be new. The prediction is confirmed by our analysis of the transcriptomes, metabolomes and mortality curves for populations of *D. melanogaster* on sugar-rich diets and mortality curves for very large cohorts of medflies [21]. We establish specific metabolites and genes as be biomarkers of ageing in *D. melanogaster*, the respective human orthologs, and provide their associations with genes and pathways commonly related to the major diseases of elders.

We show that the dynamics of ageing, as manifested in transcriptional and metabolic profiles, contains both a stochastic component, related to regulatory error accumulation in transcription/translation/metabolic pathways, and a strong deterministic component, which can be naturally associated with a development programme and leads to ageing in a form of hyperfunction. We conclude on this basis that the error accumulation and the programmed ageing hypotheses may, in fact, be compatible with each other. We show the presented model may serve to embrace most of the known features of the ageing processes and hence can emerge as a novel and universal way for quantitative ageing characterization. We believe that the theoretical ideas presented in the Letter be useful in identification of biomarkers and, after a proper development, mechanistic level processes regulating ageing in any sufficiently long lived organisms.

RESULTS

Age-associated stochastic dynamics of transcriptional and metabolic profiles. Quantitative model of ageing

In this Section we first explain the theoretical basis for our quantitative analysis of transcriptional and metabolic profile changes with age and construct the quantitative model of ageing. We consider the case of a gene regulatory network (GRN in what follows) described by a generic set of non-linear matrix equations of systems biology, $f(x, dx/dt, d^2x/dt^2, \dots) = F$. Here f is a vector function of any number of quantities representing the state of the system, x , and its time derivatives, which characterizes the interactions between different components of x , and the vector F describes the action of mostly stochastic external or endogenous stress factors affecting the gene expression levels. If, for example, the state vec-

tor x consists of the gene expression levels only, as in *e.g.* [19], the functions f may be thought as encoding pathways, which the given genes contribute to. The vector F may depend on time, t : $F(t) = F_0 + \delta F(t)$, where F_0 and δF represent the mean stress and the fluctuations of stress levels, respectively. In addition to gene expression levels, the state vector x may include other descriptors, [19], such as levels of metabolites [20] or methylation levels on CpG sites [22]. As the system state vector x is not observable in its entirety, we presume that any sufficiently large part of it captures a sufficient amount of information about the biological system state (and the dynamics of ageing).

Over long times, gene expression levels typically fluctuate near certain, relatively slowly changing, mean values, corresponding to the homeostatic state of an organism. Therefore, we assume that there always exists a quasi-stationary point x_0 (homeostasis of the organism), given by the solution of the stationary equation $f(x_0) = F_0$. As a result, the slow dynamics of the fluctuations of the gene expression levels, $\delta x = x - x_0$, follows in its leading order the matrix stochastic equation of a linear (continuum-limit) Markov chain:

$$D\delta\dot{x} + K\delta x = \delta F, \quad (1)$$

where the matrices D and K correspondingly describe the dynamical relaxation properties of the gene expression levels and the interactions between the components of the gene regulatory network (see Supplementary Information, Section A for the in-depth derivation of Eq. (1)).

It has been previously suggested that in most species GRNs operate close to a stability-instability or order-disorder bifurcation [23, 24]. The transition from stability to instability in networks with network graphs not possessing specific symmetries is typically associated with existence of co-dimension 1 bifurcations [25, 26]. Such transitions are characterized by the loss of stability along a single principal component of the network state vector, while contributions from all other principal components remain stable. This situation, known in the literature as a saddle-node bifurcation [25], is realized when the lowest (real) eigenvalue, ϵ , of the regulatory network matrix K reaches zero, $\epsilon \rightarrow 0$, and then becomes negative. Accordingly, the stationary solution for x_0 ceases to exist, and the homeostatic state of the organism starts to change in time. As we shall argue, this very instability may be directly responsible for the process of ageing.

As explained in Supplementary Information A, close to the co-dimension 1 bifurcation point the dynamics of the gene expression levels δx becomes critical. This implies that fluctuations of the expressome δx are strongly amplified with age, the phenomenon known as critical slowing-down, see *e.g.* [27]. In particular, the autocorrelation time scale $t_{\text{auto}} = (a^T \cdot Db)/\epsilon$ of the expressome diverges at $\epsilon \rightarrow 0$, implying that stochastic dynamics of δx becomes very slow near the point of bifurcation. The fluctuations of the expressome state vector δx in-

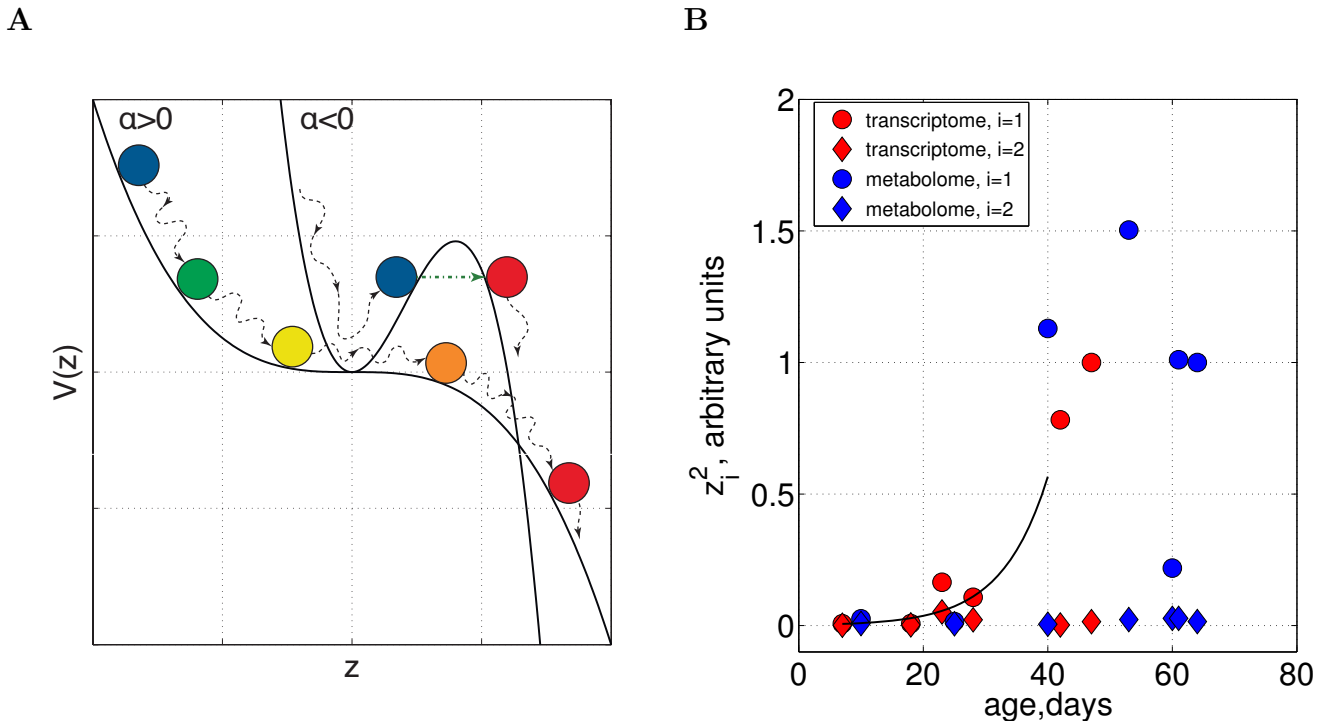


Figure 1: (A) Schematic representation of the stochastic dynamics in the effective potential $V(z)$ corresponding to the cases of stable ($\alpha > 0$) and unstable ($\alpha < 0$) GRNs, see Eq. (2). (B) Age dependence of the variance, $E(z_{1,2}^2)$, $z_{1,2} = (\delta x^T \cdot b_{1,2})$, $i = 1, 2$, of the expressome state projections onto the first two principle component vectors $b_{1,2}$ as functions of age (gene expressions from [19], red, and metabolites levels from [20], blue). Here $E(\dots)$ stands for the average over the biological repeats; $(a^T \cdot b)$ denotes a scalar product of two vectors a and b .

cluding those created in response to persistent external stress are mostly amplified along the direction b of the right eigenvector of K corresponding to the vanishing eigenvalue ϵ [28]. This, in turn, guarantees, that over very long times comparable to the average lifespan the gene expression dynamics is dominated by the single principal component collinear with the direction of the vector b . We conclude that the fluctuations of the GRN state vector δx evolving over long intervals of time can be accurately described with the help of a single variable z , such that $\delta x \approx z \cdot b$. Accordingly, Eq. (1) can be reduced to the equation

$$\frac{dz}{dt} + \frac{\partial V(z)}{\partial z} = f, \quad (2)$$

describing the Brownian motion of a particle in an effective potential $V(z) \approx -\alpha z^2/2$, where the quantity $\alpha = -\epsilon/(a^T \cdot Db)$ characterizes the “stiffness” of the gene regulatory network. The stochastic force, $f = (a^T \cdot \delta F)/(a^T \cdot Db)$, is a single unified quantitative measure of all external and endogenous “genotoxic” stress, and is characterized by the diffusion coefficient Δ (see Supplementary Information A for the in-depth derivation and discussion).

Depending on the specific morphological properties of the gene regulatory network, the curvature of $V(z)$ at

small z can be negative, $\alpha < 0$, or positive, $\alpha > 0$, as shown on Figure 1A. In the latter case, the GRN is inherently unstable, and the variance of the gene expression levels, $C(t)$, computed using the solutions of Eq. (2) grows exponentially with age as

$$C(t) = E(\delta x(t)\delta x^T(t)) \approx E(\delta x_0^2)b \cdot b^T \exp(2\alpha t). \quad (3)$$

The expression (3) is fully consistent with earlier observation of increasing biological variability with age [29, 30].

Criticality of the dynamics of gene expression levels implies that the parameter α is small and hence the covariance matrix $C(t)$ of the expressome should be very singular. The right eigenvector of the covariance matrix corresponding to its largest eigenvalue coincides in this case with the right eigenvector b of the matrix K corresponding to vanishing eigenvalue $\epsilon \rightarrow 0$ (see Supplementary Information, Section A).

These conclusions are supported by Principal Components Analysis (PCA) of the age-dependent shifts of RNA transcript and metabolite levels in *D. melanogaster* from [19] and [20], respectively. The covariance matrices computed from such datasets are indeed very singular, see Supplementary Information, Figure 4. This means that the dynamics of the state vector δx is dominated by the variance along the first principal component, $z \equiv z_1$,

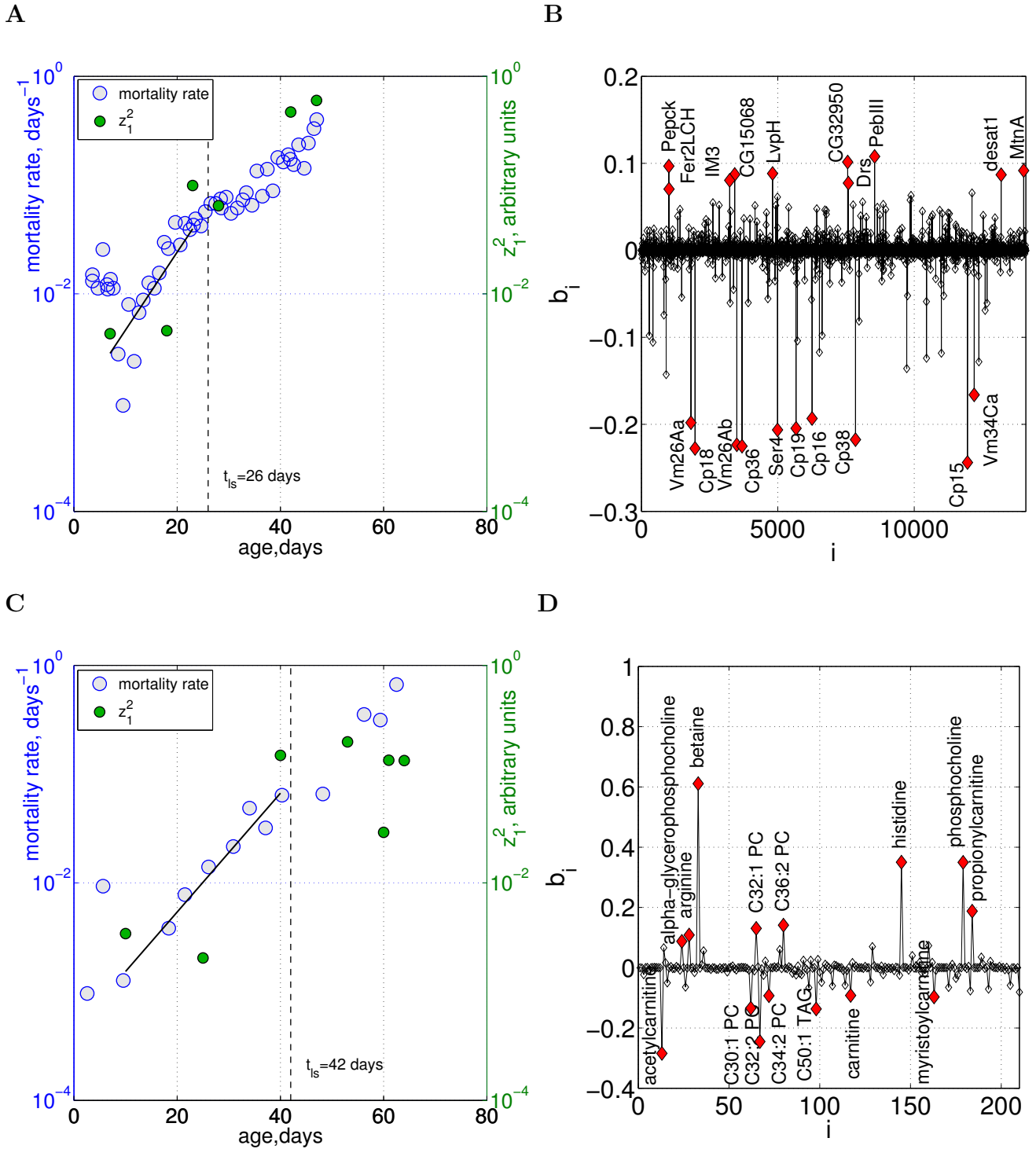


Figure 2: Basic biological evidence for the presented stochastic model of ageing: (A) The mortality along with the projection z of the system state vector, δx , represented by the transcriptomes of ageing *D. melanogaster* [19], onto the singular direction b of the covariance matrix $E(\delta x(t)\delta x^T(t'))$ as a function of age. (B) Components of the vector b for *D. melanogaster*, analysis of age-associated changes in transcriptional profiles only. Peaks correspond to the values of the components of the vector b for every gene in the dataset. (C) The mortality and the projection z of the system state vector δx , represented by the metabolomes of ageing *D. melanogaster* [20]; (D) Components of the vector b for *D. melanogaster*, computed using the levels of targeted metabolites only [20].

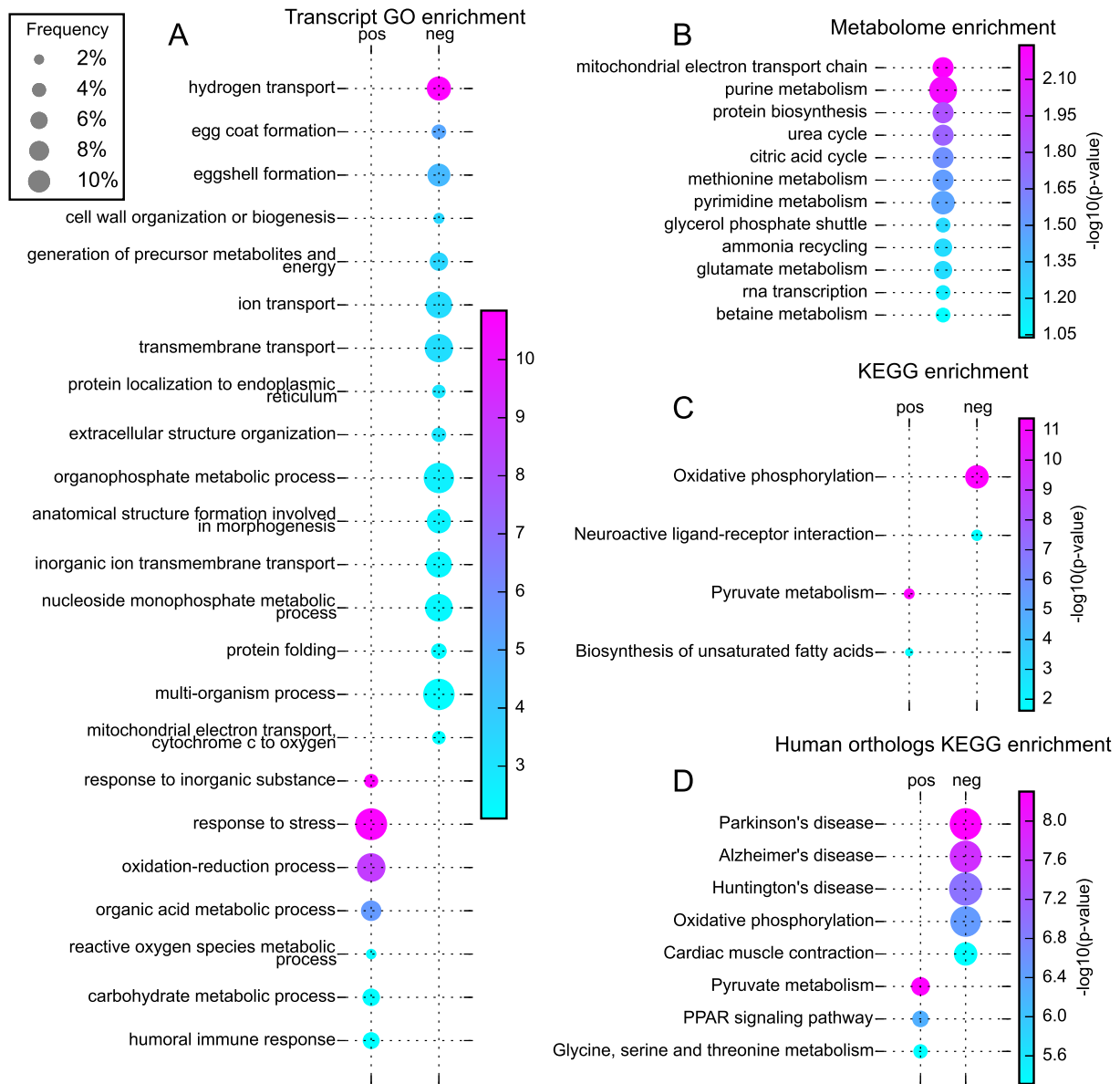


Figure 3: Biological characterization of the “leading direction of ageing” b in *D. melanogaster*: (A) Gene Ontologies (Biological Process only) enrichment by the leading positive and negative components of the vector b computed using the gene expressions; (B) Metabolite set enrichment for the leading components of the vector b computed using the levels of targeted metabolites; (C) KEGG pathways enrichment by the gene sets representing the leading components of b , corresponding to positively and negatively regulated genes; (D) KEGG pathways enrichment by human orthologs of the ageing direction in fruit flies.

where $PC_1 = (\delta x^T \cdot b_1)$, as described on Figure 1B. The variance along PC_1 grows exponentially with age, both in metabolome and in the transcriptome, in accordance with Eq. (3). The exponent, roughly inferred from each of the datasets for ages less than the mean lifespan, appears to be nearly constant, which is an indication of the same GRN instability observed in each of the measurements. For the sake of comparison, we have also plotted projections of the gene expressions on the next principal

component, PC_2 . It is easy to see that the transcriptome remains dynamically stable along PC_2 , exactly as expected from an unstable GRN near a co-dimension 1 saddle-node bifurcation, governed by Eq. (2). We thus conclude that at the origin, $z \approx 0$, the expressive state corresponds to a healthy or a “youthful” state, while the larger values of z phenotypically describe transcriptionally distorted states of aged animals. Accordingly, ageing manifests itself as a slow dynamics of gene expression

levels, a “simple” exponential roll-out along the singular, or “ageing” direction b , from the younger animals to the older ones. The singular “direction of ageing” b is associated with a response to a generic stress and determined by the properties of the gene interactions only. Since, at least within the model assumptions, the direction b does not depend on the genotoxic stress factors and appears to hard-coded in the genome, the development of an organism along “the direction of ageing” b may be said to be governed by a gene-encoded program (or a quasi-program [31–34]).

Gompertz mortality law and biological age.

To causally relate the GRN instability with the process of ageing we further assume, in a way consistent with hyperfunction hypothesis [5], that for every gene in the genome there exists a particular threshold Z_i of its expression, which is associated with a strong build-up of toxicity in associated pathways, such as *e.g.*, generation of Reactive Oxygen Species (ROS), and a subsequent inevitable death of a specimen. After the projecting of the expressome δx on the leading principal component $\sim b$ most information about the geometry of this “threshold surface” is of course lost. Nevertheless it is reasonable to assume that the death of an organism occurs once the projection $z = (b^T \cdot \delta x)$ reaches a certain threshold, $z = Z$.

If the limiting toxicity occurs late in life, *i.e.* if $\gamma = \alpha Z^2 / \Delta \gg 1$, the mortality grows exponentially at intermediate ages, $\alpha^{-1} \lesssim t \lesssim t_{ls}$ (where t_{ls} is the average lifespan in the population),

$$M \approx 0.61\alpha e^{\alpha(t-t_{ls})} \sim \frac{\Delta}{Z^2} e^{\alpha t}, \quad (4)$$

which is, essentially a form of the Gompertz law[35] (see Supplementary Information, Section B for the details of the derivation). Therefore the exponent α is directly related to the Mortality Rate Doubling Time (MRDT), t_{MRDT} , by equation $\alpha = \log(2)/t_{MRDT}$. In turn, the Initial Mortality Rate (IMR), Λ_{IMR} , is related to the genotoxic stress levels, $\Lambda_{IMR} = \Delta/Z^2$. Normally, $\gamma \sim (\alpha/\Lambda_{IMR})$ is large, and therefore average lifespan, $E(t_{ls}) \sim \alpha^{-1} \log \gamma \gg \alpha^{-1}$, is also large compared to the characteristic time $t_\alpha \sim \alpha^{-1}$ associated with the gene network instability. The lifespan thus depends strongly on the morphological properties of the GRN, such as its topology and connectivity, through the matrix K , and, more specifically, through its lowest eigenvalue $\epsilon \sim \alpha$. The dependence of species lifespan on the genotoxic stress factors through the parameter Δ is, on the contrary, logarithmically weak. This may explain why interventions aimed at insulating a living system from stress, *e.g.* by regulating the environmental temperature or by decreasing ROS levels alone, failed to dramatically improve lifespan [36].

Mortality in the form similar to Eq. (4) can be associated with the gene network instability in a simple phenomenological model, where both IMR and MRDT were related to generic network parameters, such as translation, gene repair and protein turnover rates, along with the genotoxic stress levels, whereas mortality was directly associated with the increasing number of regulatory errors [17]. Therefore the expressome remodeling along the ageing direction b can be related to the total unrepaired damage accumulated over the lifespan of an organism.

As we show in Supplementary Information, the dynamics of gene expression levels δx in a strong “Gompertzian” limit, $\gamma \gg 1$, proceeds along a well-defined trajectory, corresponding to a continuation of the development program. This conclusion is entirely consistent with the hyperfunction hypothesis [5] as a special case of pre-programmed ageing. The “distance travelled” along the ageing direction up to a date, $z \sim (\delta x^T \cdot b)$, is, according to Eq. (4), directly related to mortality and hence by itself is a good biomarker of mortality and ageing. These observations pave the way to define a number of biological “clocks” using any number of variables characterizing a GRN state. For example, Figures 2A & C demonstrate the feasibility of a transcriptome- and metabolome- derived biological clock for *D. melanogaster*. Those clocks in turn may be compared to the biomarkers of age and the biological age calculator (biological clock) derived from a regression model established using age-dependent DNA-methylation levels [22].

The association of GRN instability and the mortality rate

Our analysis of *D. melanogaster* age-dependent transcriptional data indicates that the gene expression variance grows exponentially with the age in agreement with Eq. (3), with $\alpha \approx 19.1 \text{ yr}^{-1}$, as shown on Figure 2A. In a similar fashion we have studied the composition of the “direction of ageing” b in metabolome of *D. melanogaster* [20] maintained on a sugar diet. The projection of the metabolome state vector onto the singular direction b increases very quickly with age, along with the reported mortality as shown on Figure 2C. The average lifespan of *D. melanogaster* is about 25 and 40 days in both experiments, respectively, and in both cases the initial exponential growth of the projection $z^2(t)$ ceases at $t \gtrsim t_{ls}$, as predicted by the theory. Figure 1B represents a side by side comparison of the variance computed from the gene expression and the metabolomes datasets. The values of instability rates, α , recovered both ways are very similar, and close to the value of the Gompertz exponent $\alpha = \ln 2 / t_{MRDT} = 17.1 \text{ yr}^{-1}$ corresponding to the mortality rate doubling time $t_{MRDT} \approx 0.04 \text{ yr}$ [37].

Mortality rate slowdown at advanced ages

At more advanced ages, $t \gtrsim E(t_{le})$, where t_{le} is the average lifespan in the population, solutions of Eq. (2) exhibit deceleration of mortality. More specifically, as shown in Supplementary Information, Section B 4 d, we expect that the mortality rate ceases growing and saturates at a constant value, $M_\infty \sim \alpha$. This quantitative prediction can be compared with the experimental data for medflies [21], where the cohort sizes were sufficient to observe both the regime of exponentially increasing mortality and the mortality plateau (see Supplementary Information, Figure 7). For the male medflies we find the asymptotic value $M_\infty \approx 0.16 \text{ day}^{-1}$, which is close to the Gompertz exponent $\alpha \approx 0.22 \text{ day}^{-1}$, as expected. The asymptotic value of the mortality rate for female medflies, $M_\infty \approx 0.12 \text{ day}^{-1}$, is also of the right order of magnitude, though nearly two times smaller than the slope of the mortality exponent $\alpha = 0.25 \text{ day}^{-1}$. Nevertheless, we emphasize the existence of a strong correlation between the asymptotic value M_∞ of the mortality rate at late ages and the value of the Gompertz exponent α in both cases and note that the approximate Eq. (4) works better for longer living, or ‘‘Gompertzian’’, $\Lambda_{IMR} \ll \alpha$, organisms.

Genes-biomarkers of ageing in *D. melanogaster*

The ‘‘direction of ageing’’, vector b , is similar but not the same as differential expression (DE) vector in ageing animals, since the latter may include a contribution of faster modes represented by the eigenvectors of the GRN connectivity matrix K corresponding to eigenvalues with larger absolute value. The results of Gene Ontology (GO) analysis of the leading components of b vector are summarized in Figure 3A, for Biological Process (BP) categories only. A summary for Molecular Function (MF) and Cellular Compartment (CC) categories enrichment can be found on Supplementary Information Figures 9B & C.

The genes, providing the most significant negative contribution to the ageing direction, b , can be roughly split into three groups. First, there is a large group of genes related to metabolic processes: organophosphate metabolism, generation of precursor metabolites and energy, membrane and mitochondria ion transport. A detailed review of the GO categories involved seem to indicate that most of the down-regulated processes are related to oxidative phosphorylation or respiration (see below). Another seemingly large group of genes involves apparent remedies of developmental processes, such as anatomical structure formation involved in morphogenesis and extracellular structure organization. Genes encoding eggshell formation, more specifically, egg coat formation, correspond to strongly negative components of the vector b , which is a clear sign of the reproductive senescence in female flies. Finally, we observe the decline

in protein folding capacity, along with an apparently related ‘‘unfolded protein binding’’ GO MF category.

As expected, the cluster of genes corresponding to the strongest positive components of the vector b includes genes associated with a generic stress response. Among other leading components are genes corresponding to humoral immune response (well in line with the earlier conclusions of [38]), and the components of oxidation-reduction and reactive oxygen species metabolic processes. The latter may be over-expressed with age in response to Reactive Oxygen Species (ROS) accumulation. This over-expression may be occurring on par with the decline of the metabolic processes. The carbohydrate metabolic processes activation may be another programmed defensive measure on the background of the oxidative phosphorylation decline (see below). This observation seems to be consistent with enrichment of KEGG oxidative phosphorylation pathway by the negative leaders of the ageing direction, see Figure 3C.

A few transcription factors (TF) expression shifts are strongly associated with ageing. The top positively associated gene, *hairy*, is a transcriptional suppressor, and believed to be a metabolic switch, found up-regulated in the microarrays characterizing oxygen-deprived flies. Conversely, mutations in *hairy* significantly reduced hypoxia tolerance [39]. This can be either a driving force behind or an indication of a pre-programmed metabolic adaptation to the oxidative phosphorylation decline. The only negatively associated transcriptional factor, *eve*, is a transcriptional factor involved in multiple organ an systems development.

Metabolites-biomarkers of ageing in *D. melanogaster*

We computed the ageing direction basing on the results of the metabolic remodeling study for *Drosophila melanogaster* [20]. Most of the metabolites, used in the analysis, are not annotated (see Supplementary Information, Figure 8). To facilitate the discussion, we also re-computed the ‘‘direction of ageing’’ b using only the targeted metabolites, see Figure 2D. The results for both targeted and non-targeted metabolites should be taken with a grain of salt, as metabolite level numbers for different metabolites resulting from metabolite profiling are not equally normalized, are not generally in one-to-one correspondence with metabolite concentrations in the live tissue, and thus levels of two different metabolites estimated by metabolite profiling strictly speaking cannot be quantitatively compared with each other. The effects of unequal normalization are especially pronounced for non-annotated metabolites. Nevertheless, the relation between targeted metabolites turned out to be the same in both analyses of the full metabolome and the annotated list only, which is a good indication of the stability of calculations and possibility to scale calculation to state vectors with more components. The issue of unequal normalization in omics datasets can be fully

resolved by applying stochastic subspace identification methods [40], which we shall leave for a future work.

The most reliable sets of enriched metabolites participating in mitochondrial electron transport chain (alpha-glycerophosphate, succinate, NAD) mainly correspond to negative components in the vector b , which is consistent with earlier reported age-associated decline in mitochondrial respiration and electron transport in *D. melanogaster* [41]. The majority of the purine metabolism category members, such as adenosine, guanosine, inosine, urate, glutamine, etc., are characterized by the negative values of the vector b as well, which is consistent with the age-related expression decline of the gene associated with major metabolic pathways (see above).

Human orthologs for biomarkers of ageing in *D. melanogaster*

According to OrthoDB, approximately 80% of all genes in *D. melanogaster* have human orthologs. To provide more quantitative insights into the nature of the ageing direction, we searched for human orthologs to the leading contributors to the ageing direction vector b computed from the transcriptome of *D. melanogaster*. The results of this analysis are represented on Figures 3C & D. A fair number of the lead components of the ageing direction, such as e.g. egg shell proteins, are clearly species dependent. At the same time the human orthologs list appears to make sense. As expected, the downregulated genes enrich KEGG pathways associated with oxidative phosphorylation (consistently with the GO annotation and KEGG enrichment results above). On top of that we find the KEGG categories corresponding to the leading age-related neurodegenerative diseases (Huntington's, Parkinson's and Alzheimer's), and also cardiac muscle contraction pathway. Heart failure is known to be another common causes of death in elders. On the contrary, KEGG PPAR signaling pathway is getting activated with age, which may be another indication of the aforementioned activation of anti-oxidant metabolism systems. There is an evidence suggesting that PPAR α and the genes under its control play a role in the evolution of oxidative stress excesses observed in the course of ageing in mice [42].

Another characteristic piece of evidence relating the stochastic instability of the gene regulatory network with common age-related diseases is a strong positive contribution of Pepck gene, which encodes a rate-controlling enzyme of gluconeogenesis, the process by which cells synthesize glucose from metabolic precursors. RNAi approach to induce post-transcriptional gene silencing of its human ortholog, PEPCK, was identified as an effective way to sustain diabetes-induced hyperglycemia [43].

DISCUSSION

We have argued in the present paper that ageing is an organismic level manifestation of an inherent instability of gene regulatory networks. Proper orthogonal decomposition of age-dependent transcriptional and metabolic profiles shows that for Gompertzian species the life-long dynamics of the transcriptional and metabolic profiles can be effectively described as a stochastic critical dynamics of a single degree of freedom, identified by the projection of the expressome on the right eigenvector b of the GRN connectivity matrix K , and associated with the eigenvalue ϵ vanishing at the critical point.

We established that depending on the sign of ϵ a GRN can be either stable or unstable. We further invoke a form of hyperfunction theory and assume that a buildup of metabolites beyond a certain lethal level leads to death of the organism. We note that appearance of such toxicity thresholds is guaranteed, if non-linearities in the equation (1) for expressome levels are accounted for (see Supplementary Information, Section B). We show that in this limit the mortality follows a form of Gompertz law, i.e. first increases exponentially with age and then saturates at a constant level, which is supported by experimental evidences. As predicted, we find a strong correlation between the rate of gene regulatory network instability and the value of mortality rate saturation. Thus we are able to demonstrate that the Gompertzian ageing is a property of organisms with inherently unstable gene regulatory networks, and thus the gene network instability is a direct cause of ageing in the form of exponential increase of all-causes mortality with age. Since mortality in humans, where it is characterized best, is, for most of its part, associated with age related diseases, our calculations support the idea of ageing being the driving force behind the development of major diseases [44].

The stochastic theory of ageing presented is fully compatible with and, in fact, embraces the existing theories and hypotheses on the origin of ageing in the following sense:

- **programme of ageing** [11–13]. We have shown that ageing-driven dynamics of the expressome $\delta x(t)$ can be separated into stochastic and deterministic components. The deterministic component of $\delta x(t)$ starts to dominate over the stochastic one already early in life, at roughly the same time when the low rank approximation of the GRN connectivity matrix K becomes valid. As the dynamics of the expressome $\delta x(t)$ is largely determined by the properties of the matrix K , we identify the low rank approximation of K as a quasi-programme of ageing.
- **hyperfunction theory** [5, 6]. The single mode $\delta x = z \cdot b$, describing a large cluster of genes provides a dominant contribution to the process of ageing, starts dominating the ageing dynamics soon after the end of the developmental stage, and the

stochastic effects on the expressive dynamics can be considered relatively weak [5, 6]. The same genes, which were highly expressed close to the end of the developmental stage, become even more over-expressed at late stages of life. Therefore it is natural to associate the progressing of $\delta x(t)$ along the ageing mode with the hyperfunction. Moreover, introduction of toxicity thresholds for metabolic profile and gene expression levels is also consistent with the idea of hyperfunction. More evidence in favor of the interpretation comes from recent works such as [45], where a specific transcriptional circuit is found, which guides the rapid ageing process in *C. elegans* and indicate that this circuit is driven by drift of developmental pathways rather than accumulation of damage.

- **damage/error accumulation** [1–4]. Although the stochastic component of expressive $\delta x(t)$ becomes small compared to the deterministic component at late ages, its effects are strongly pronounced at all ages. The probability distribution function $P(\delta x, t)$ to find a specimen with the expressive $\delta x(t)$ and age t in a population is never peaked near a particular value of δx . On the contrary, we have argued in the present paper, that the mean square deviation $\sqrt{E(\delta x^2(t))}$ grows with age at the same exponential Gompertz rate as the mortality $M(t)$. As we will demonstrate in the future work, this growth of stochasticity in population can be directly associated with the effect of error accumulation in metabolism and gene regulation through the estimation of entropy growth rate, as has been earlier suggested by [46, 47].
- **antagonistic pleiotropy** [9]. Since a single mode $\delta x = z \cdot b$ determines the dynamics of the expressive $\delta x(t)$ through the most of the adult life, expression levels of the genes, highly expressed in the end of developmental stage, will first reach toxicity thresholds leading to statistical increase of mortality. Such highly expressed genes are clearly selected for, as they promote the fitness of the organism in youth. This observation is very much in the spirit of the hypothesis of antagonistic pleiotropy.

The established relation between the critical dynamics of the gene regulatory network state vector and the Gompertzian mortality characteristic to many species allows one to consider the projection $z = (b^T \cdot \delta x)$ as a biomarker of ageing. Due to the low value of the eigenvalue ϵ the direction b dominates a response to a generic stress. This, in fact, was already demonstrated in [48], where transcriptional signatures of responses to very different genotoxic stresses were found to share a great number of gene expression changes.

The expressions of the genes or metabolites corresponding to the most significant components of the ageing direction b are strongly associated with age and age related diseases. Therefore ageing in the form the GRN

instability described here leads to the impairment of the normal functioning of the body, has characteristic biomarkers and symptoms including signs of major age related diseases, and produces exponentially increasing morbidity. Accordingly, the process of ageing itself falls under the definition of a disease recently used by AMA for a common condition such as obesity [49]. We must note here that therapeutic or experimental interventions aimed to counter-balance the age related changes in the genes or metabolites expressions may not be very effective ways to extend lifespan of the species. For example, even though ageing in *D. melanogaster* is associated with increased internal and external bacterial load, as well as with increase of antibacterial peptides expression, both reducing the bacteria population with antibiotics and reducing the humoral antibacterial response failed to induce lifespan increasing effect in experiments [50]. The transcriptional factor *hairly* is overexposed with age, nevertheless its inhibition did not result in lifespan increase either [39]. This reinforces the conclusion that the markers of ageing are, in general, not the same as regulators of ageing.

Even though most of the analysis in the manuscript is performed for *D. melanogaster*, our conclusions are generic and should be applicable to other species. Realistic GRNs with different properties may not lead to Gompertz law. We believe that even more intriguing possibility may arise if the effective potential $V(z)$ has a local minimum with small but positive curvature. The higher order nonlinearities, such as cubic component of the effective potential, cannot be neglected anymore and in this case genetic network turns out to be metastable. If the minimum of the potential $V(z)$ is separated from the region of large z by a sufficiently high activation barrier (see Figure 1A and Supplementary Information, Section B 5 c), the mortality rate, determined by the probability of activation, is exponentially small and age-independent. This situation is consistent with the negligible senescence hypothesis [51]. This model feature may provide an explanation behind the apparent lack of age-dependent physiological changes as well as behavior of the mortality rate observed in naked mole rat and some other species over a long lifespan [52]. This argument is also supported by the analysis in [53], where the number of the genes differentially expressed with the age was compared in naked mole rats, mice, and humans [53, 54].

MATERIALS AND METHODS

Gene annotation

We have used the open source Ontologizer [55] tool to annotate the gene set representing the leading components of the vector b of biomarkers of ageing. The vector b was first computed from the gene expression variance to gene ontologies using “Parent-Child-Intersection” GO enrichment analysis procedure described in [56], a

method, which considers genes in the background if they are present in all parent terms of the term of interest. For comparison purposes we also present a standard Term-by-Term GO enrichment (BP only) analysis on Supplementary Information Figures 9A. We employed 0.01 adjusted p -value cutoff (Benjamini-Hochberg multiple test correction). We have performed KEGG pathway enrichment analysis of the genes corresponding to the most significant components of vector b , computed from the transcriptome of *D. melanogaster* [19] and the corresponding human orthologs using DAVID web-tool [57, 58].

Metabolic enrichment analysis

To analyze the vector b , obtained from the metabolome of *D. melanogaster* [20], we have performed a metabolite

set enrichment analysis for the components of vector b using MetaboAnalyst 3.0 [59]. The total number of the targeted metabolites is too small to analyze the positively and negatively regulated substances separately. 80 components of the vector b with highest absolute value are represented on Figure 3B.

ACKNOWLEDGMENTS

The authors are grateful to Profs. A. Moskalev, V. Gladyshev and V. Fontana, Drs. A. Avanesov and M. Konovalenko for valuable discussions, Dr. U. Fischer and to S. Filonov and M. N. Kholin for enlightening comments, discussions and substantial help in preparation of the manuscript. We would also like to thank Prof. J. Carey for access to the experimental data.

-
- [1] Partridge, L. & Gems, D. Mechanisms of ageing: public or private? *Nat. Rev. Genet.* **3**, 165–75 (2002). URL <http://dx.doi.org/10.1038/nrg753>.
- [2] Sinclair, D. A. & Oberdoerffer, P. The ageing epigenome: damaged beyond repair? *Ageing Res. Rev.* **8**, 189–98 (2009). URL <http://www.sciencedirect.com/science/article/pii/S1568163709000245>.
- [3] Gladyshev, V. N. On the cause of aging and control of lifespan: heterogeneity leads to inevitable damage accumulation, causing aging; control of damage composition and rate of accumulation define lifespan. *Bioessays* **34**, 925–9 (2012).
- [4] Gladyshev, V. N. The origin of aging: imperfectness-driven non-random damage defines the aging process and control of lifespan. *Trends Genet.* **29**, 506–12 (2013).
- [5] Blagosklonny, M. V. Aging and immortality: quasi-programmed senescence and its pharmacologic inhibition. *Cell Cycle* **5**, 2087–2102 (2006).
- [6] Blagosklonny, M. V. & Hall, M. N. Growth and aging: a common molecular mechanism. *Aging* **1**, 357 (2009).
- [7] Kirkwood, T. B. L. Evolution of ageing. *Nature* **270**, 301–304 (1977).
- [8] Kirkwood, T. B. & Austad, S. N. Why do we age? *Nature* **408**, 233–8 (2000).
- [9] Williams, G. Pleiotropy, natural selection, and the evolution of senescence. *Science's SAGE KE* **2001**, 13 (2001).
- [10] Reis, R. J. S. Model systems for aging research: syncretic concepts and diversity of mechanisms. *Genome* **31**, 406–412 (1989).
- [11] Skulachev, V. The programmed death phenomena, aging, and the Samurai law of biology. *Exp. Gerontol.* **36**, 995–1024 (2001).
- [12] Longo, V. D., Mitteldorf, J. & Skulachev, V. P. Programmed and altruistic ageing. *Nat. Rev. Genet.* **6**, 866–72 (2005).
- [13] de Magalhães, J. a. P. Programmatic features of aging originating in development: aging mechanisms beyond molecular damage? *FASEB J.* **26**, 4821–6 (2012). URL <http://www.fasebj.org/content/26/12/4821.short>.
- [14] Orgel, L. E. Ageing of Clones of Mammalian Cells. *Nature* **243**, 441–445 (1973).
- [15] Hopfield, J. J. Kinetic Proofreading: A New Mechanism for Reducing Errors in Biosynthetic Processes Requiring High Specificity. *Proc. Natl. Acad. Sci.* **71**, 4135–4139 (1974).
- [16] Danchin, A. Natural selection and immortality. *Biogerontology* **10**, 503–16 (2009).
- [17] Kogan, V., Molodtsov, I., Menshikov, L. I., Reis, R. J. S. & Fedichev, P. Stability analysis of a model gene network links aging, stress resistance, and negligible senescence. *arXiv preprint arXiv:1408.0463* (2014).
- [18] Antoulas, A. C. *Approximation of Large-Scale Dynamical Systems* (SIAM, 2009).
- [19] Pletcher, S. D. *et al.* Genome-wide transcript profiles in aging and calorically restricted *Drosophila melanogaster*. *Current Biology* **12**, 712–723 (2002).
- [20] Avanesov, A. S. *et al.* Age- and diet-associated metabolome remodeling characterizes the aging process driven by damage accumulation. *eLife* **3** (2014).
- [21] Vaupel, J. W. *et al.* Biodemographic trajectories of longevity. *Science* **280**, 855–860 (1998).
- [22] Horvath, S. Dna methylation age of human tissues and cell types. *Genome biology* **14**, R115 (2013).
- [23] Balleza, E. *et al.* Critical dynamics in genetic regulatory networks: examples from four kingdoms. *PLoS One* **3**, e2456 (2008).
- [24] Krotov, D., Dubuis, J. O., Gregor, T. & Bialek, W. Morphogenesis at criticality. *Proceedings of the National Academy of Sciences* **111**, 3683–3688 (2014).
- [25] Fiedler, B. E. *Handbook of Dynamical Systems, Volume 2* (Gulf Professional Publishing, 2002).
- [26] Seydel, R. *Practical Bifurcation and Stability Analysis*, vol. 1 (Springer Science & Business Media, 2009).
- [27] Suzuki, M. Passage from an initial unstable state to a final stable state. In *Advances in Chemical Physics, Volume 46*, 195–276 (John Wiley & Sons, 2009). URL <http://books.google.com/books?hl=en&lr=&id=6uAY7tkKEVcC&pgis=1>.
- [28] The latter observation is supported by the analysis of the recent experiments in *D. melanogaster*, where transcriptional responses to different stress factors were found to contain a good fraction of similar differentially expressed

- genes both in the limit of nearly lethal [60] and weak stressors [48].
- [29] Morse, C. Does variability increase with age? an archival study of cognitive measures. *Psychol Aging* **8**, 156–64 (1993).
- [30] Rother, P. The aging changes of biological variability (author’s transl). *ZFA* **33**, 463–6 (1978).
- [31] Khalyavkin, A. & Krutko, V. Aging is a simple deprivation syndrome driven by a quasi-programmed preventable and reversible drift of control system set points due to inappropriate organism-environment interaction. *Biochemistry (Moscow)* **79**, 1133–1135 (2014).
- [32] Arlia-Ciommo, A., Piano, A., Leonov, A., Svistkova, V. & Titorenko, V. I. Quasi-programmed aging of budding yeast: a trade-off between programmed processes of cell proliferation, differentiation, stress response, survival and death defines yeast lifespan. *Cell Cycle* **13**, 3336–3349 (2014).
- [33] Blagosklonny, M. V. Answering the ultimate question" what is the proximal cause of aging?". *Aging* **4**, 861–877 (2012).
- [34] Blagosklonny, M. V. Mtor-driven quasi-programmed aging as a disposable soma theory. *Cell Cycle* **12**, 1842–1847 (2013).
- [35] Gompertz, B. On the nature of the function expressive of the law of human mortality, and on a new mode of determining the value of life contingencies. *Philosophical transactions of the royal society of London* **115**, 513–583 (1825).
- [36] Gems, D. & Doonan, R. Antioxidant defense and aging in *c. elegans*: is the oxidative damage theory of aging wrong? *Cell Cycle* **8**, 1681–1687 (2009).
- [37] Tacutu, R. *et al.* Human ageing genomic resources: Integrated databases and tools for the biology and genetics of ageing. *Nucleic acids research* **41**, D1027–D1033 (2013).
- [38] Khan, I. & Prasad, N. The aging of the immune response in *drosophila melanogaster*. *The Journals of Gerontology Series A: Biological Sciences and Medical Sciences* **68**, 129–135 (2013).
- [39] Zhou, D. *et al.* Mechanisms underlying hypoxia tolerance in *drosophila melanogaster*: hairy as a metabolic switch. *PLoS genetics* **4**, e1000221 (2008).
- [40] Overschee, V. & Moor, D. *Subspace Identification for Linear Systems: Theory, Implementation, Applications* (Kluwer Academic, 1996).
- [41] Ferguson, M., Mockett, R., Shen, Y., Orr, W. & Sohal, R. Age-associated decline in mitochondrial respiration and electron transport in *drosophila melanogaster*. *Biochem. J* **390**, 501–511 (2005).
- [42] Poynter, M. E. & Daynes, R. A. Peroxisome proliferator-activated receptor α activation modulates cellular redox status, represses nuclear factor- κ b signaling, and reduces inflammatory cytokine production in aging. *Journal of Biological Chemistry* **273**, 32833–32841 (1998).
- [43] Gómez-Valadés, A. G. *et al.* Overcoming diabetes-induced hyperglycemia through inhibition of hepatic phosphoenolpyruvate carboxykinase (gtp) with rna. *Molecular Therapy* **13**, 401–410 (2006).
- [44] Blagosklonny, M. V. Validation of anti-aging drugs by treating age-related diseases. *Aging* **1**, 281 (2009).
- [45] Budovskaya, Y. V. *et al.* An elt-3/elt-5/elt-6 gata transcription circuit guides aging in *c. elegans*. *Cell* **134**, 291–303 (2008).
- [46] Hayflick, L. Entropy explains aging, genetic determinism explains longevity, and undefined terminology explains misunderstanding both. *PLoS Genet.* **3**, e220 (2007).
- [47] Christensen, K., Doblhammer, G., Rau, R. & Vaupel, J. W. Ageing populations: the challenges ahead. *Lancet* **374**, 1196–208 (2009). URL <http://www.sciencedirect.com/science/article/pii/S0140673609614604>.
- [48] Moskalev, A. *et al.* Mining gene expression data for pollutants (dioxin, toluene, formaldehyde) and low dose of gamma-irradiation. *PLoS ONE* **9**, e86051 (2014). URL <http://dx.doi.org/10.1371/journal.pone.0086051>.
- [49] American medical association, resolution 420 (a-13): recognition of obesity as a disease. In *Proceedings of the House of Delegates 162nd Annual Meeting* (2013).
- [50] Ren, C., Webster, P., Finkel, S. E. & Tower, J. Increased internal and external bacterial load during *drosophila* aging without life-span trade-off. *Cell metabolism* **6**, 144–152 (2007).
- [51] Finch, C. E. *Longevity, senescence, and the genome* (University of Chicago Press, 1994).
- [52] Buffenstein, R. The naked mole-rat: a new long-living model for human aging research. *The Journals of Gerontology Series A: Biological Sciences and Medical Sciences* **60**, 1369–1377 (2005).
- [53] Kim, E. B. *et al.* Genome sequencing reveals insights into physiology and longevity of the naked mole rat. *Nature* **479**, 223–227 (2011).
- [54] Jeannette Loram, A. B. Age-related changes in gene expression in tissues of the sea urchin *strongylocentrotus franciscanus*. *Mechanisms of Ageing and Development* **133**, 338–347 (2012).
- [55] Bauer, S., Gagneur, J. & Robinson, P. N. Going bayesian: model-based gene set analysis of genome-scale data. *Nucleic acids research* **38**, 3523–3532 (2010).
- [56] Grossmann, S., Bauer, S., Robinson, P. N. & Vingron, M. Improved detection of overrepresentation of gene-ontology annotations with parent-child analysis. *Bioinformatics* **23**, 3024–3031 (2007).
- [57] Da Wei Huang, B. T. S. & Lempicki, R. A. Systematic and integrative analysis of large gene lists using david bioinformatics resources. *Nature protocols* **4**, 44–57 (2008).
- [58] Huang, D. W., Sherman, B. T. & Lempicki, R. A. Bioinformatics enrichment tools: paths toward the comprehensive functional analysis of large gene lists. *Nucleic acids research* **37**, 1–13 (2009).
- [59] Xia, J., Mandal, R., Sinelnikov, I. V., Broadhurst, D. & Wishart, D. S. Metaboanalyst 2.0—a comprehensive server for metabolomic data analysis. *Nucleic acids research* **40**, W127–W133 (2012).
- [60] Brown, J. B. *et al.* Diversity and dynamics of the *drosophila* transcriptome. *Nature* (2014).
- [61] Kadish, I. *et al.* Hippocampal and cognitive aging across the lifespan: a bioenergetic shift precedes and increased cholesterol trafficking parallels memory impairment. *The Journal of Neuroscience* **29**, 1805–1816 (2009).
- [62] The number of different principal components PC_n representing the signal $x(t_1), \dots, x(t_m)$ does not exceed m .
- [63] Schervish, M. J. *Theory of Statistics*, vol. 21 (Springer New York, 2011).
- [64] In particular, the rate of these changes is limited by a single gene transcription time, ~ 1 min.

- [65] In particular, they are not small at early times, close to the initial state of the expressome.
- [66] When higher order derivatives in Eq. (A1) are taken into account, this argument, albeit becoming more involved, remains valid: one has to construct the perturbation theory in powers of small parameter ϵ , which still determines the smallest eigenvalue of the matrix $A(f) = K + i2\pi fD + (2\pi f)^2 M + \dots$. Similarly to the case considered here, all higher eigenvalues of $A(f)$ possess positive real parts.
- [67] Zwanzig, R. *Nonequilibrium Statistical Mechanics* (Oxford University Press, USA, 2001).
- [68] Of course, albeit natural, this is still an assumption, as different gene expressions are not truly independent GRN state variables.
- [69] Suzuki, M. Scaling theory of transient phenomena near the instability point. *Journal of Statistical Physics* **16**, 11–32 (1977). URL <http://link.springer.com/10.1007/BF01014603>.
- [70] Redner, S. *A Guide to First-Passage Processes* (Cambridge University Press, 2001).
- [71] Aalen, O., Borgan, O. & Gjessing, H. *Survival and Event History Analysis: A Process Point of View* (Springer, 2008).
- [72] Weitz, J. S. & Fraser, H. B. Explaining mortality rate plateaus. *Proc. Natl. Acad. Sci. U. S. A.* **98**, 15383–6 (2001).
- [73] Steinsaltz, D. & Evans, S. N. Markov mortality models: implications of quasistationarity and varying initial distributions. *Theor. Popul. Biol.* **65**, 319–37 (2004).

SUPPLEMENTARY INFORMATION

Appendix A: Stochastic dynamics of gene expression and metabolic levels

In the following, we explain the physical basis for Eq. (2) and provide its derivation. We also explicitly find the expressions for the mortality rate, the survival probability, the lifespan distribution function and the average lifespan of species with expressome subject to Eq. (2).

1. Getting a grasp on the dynamics of expressome. Model reduction and physical considerations

The analysis represented in this paper is mainly based on the observation that time series datasets describing changes of expressome profiles with age are often well susceptible to Model Reduction techniques [18]. One of such methods often used in Big Data analysis is proper orthogonal decomposition (POC).

Applying POC to age-associated transcriptional and metabolic profile dynamics datasets (for example, [19, 20, 61]) shows that the long-time behavior of the expressome x is largely determined by a single principal component (see Fig. 4). Although the number of time snapshot points in corresponding time series is typically limited, [62] clear dominance of PC_1 in the signal is a non-trivial fact. As we argue here, it carries an important information about biological gene regulatory and metabolic networks; namely, it shows that such networks are pre-critical in the sense, which will be explained below.

Consider a meta-stable gene regulatory network (GRN) with the instantaneous network state represented by a vector x , whose components x_i are given by expression levels of different genes, proteins or metabolites participating in the GRN.

Dynamics of the vector x is affected by mRNA levels, concentrations of proteins and metabolites, involved in regulatory pathways and in are in turn influenced by external as well as endogenous stress factors acting on the cell. This dynamics is governed by differential matrix equations of systems biology

$$g\left(x, \frac{dx}{dt}, \frac{d^2x}{dt^2}, \dots\right) = F, \quad (\text{A1})$$

where g is a vector function of the state vector x , encoding interactions between different components of the expressome, where the notations and variables are introduced in the main text of the paper.

Generally, the vector function g may depend on arbitrarily high time derivatives $\frac{dx}{dt}, \frac{d^2x}{dt^2}, \dots, \frac{d^n x}{dt^n}, \dots$ of the expressome state vector. Hereinafter the focus is on the study of dynamics of x at time scales comparable to the mortality rate doubling time t_{MRDT} , which is of the order of tens of days for nematodes and drosophilae, and is

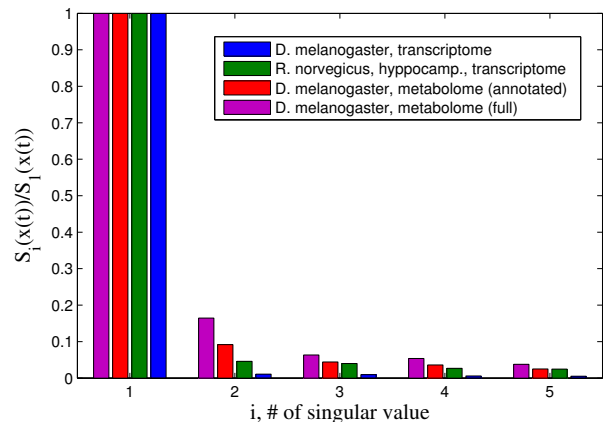


Figure 4: Five largest singular values $S_i(x(t))$ of the expressome $x(t)$ divided by the largest one, $S_1(t)$; transcriptome of *D. melanogaster* [19] (blue), transcriptome of *R. norvegicus*, hippocampus [61] (green), metabolome of *D. melanogaster*, targeted metabolites only [20] (red), metabolome of *D. melanogaster*, all metabolites [20] (purple). One of the principal components of the expressome $x(t)$ clearly dominates over the others in all considered cases.

even larger, hundreds of days, for mice. This time scale is to be compared to a typical time scale of protein translation and regulation, or a life time of mRNA, encoded in the dynamics of the vector F . In order to describe this *slow* dynamics of the expressome state vector x , one can neglect all time derivatives of x higher the first derivative $\frac{dx}{dt}$. The matrix Eq. (A1) thus reduces to

$$g\left(x, \frac{dx}{dt}\right) = F. \quad (\text{A2})$$

2. Frequency domain properties of the vector F of stress factors

As was explained above, the vector F of environmental and endogeneous stress factors affecting gene expression levels x has both slowly changing component, $F_0(t)$, and stochastic component, $\delta F(t)$, rapidly changing in time. Below we assume for simplicity that $F_0(t) = F_0$, i.e., slowly changing component is in fact constant.

Since dynamics of the vector δF can be considered essentially random at time scales of interest for us, dynamics of x is driven by correlation properties of δF . The total number of environmental and internal stress factors affecting gene expression levels x is extremely large, and the vector $\delta F(t)$ represents a superposition of these factors. According to the central limit theorem [63] it can thus be considered a Gaussian stochastic process, so that

$$E(\delta F(t)\delta F(t')) = B(t - t'),$$

where $B(t-t')$ is a function of the time difference $|t-t'|$ only, while $E(\dots)$ as usual denotes the expectation value of the fluctuating quantity \dots , and statistical average is understood as average over ensemble of species/cells of a given organism. In the frequency domain, one has correspondingly

$$\begin{aligned} E(\delta F(f)\delta F(-f)) &= \\ &= \int df e^{-2\pi if(t-t')} E(\delta F(t)\delta F(t')) = B(f), \end{aligned}$$

where f is frequency of a given mode in the Fourier expansion of the function $B(t-t')$.

The function $B(f)$ has multiple singularities in the complex plane of f . These singularities encode characteristic time scales of pathways' dynamics. However, the two following observations are important for the subsequent analysis. First of all, the function $B(f)$ decays quickly with f as $f \rightarrow \infty$. This guarantees that the amount of stress affecting the gene expression levels x does not change very rapidly.[64] On the other hand, the behavior of $B(f)$ is smooth at very small frequencies, i.e., $B(f) \rightarrow B$ as $f \rightarrow 0$, so that the amplitude of rare fluctuations of δF remains limited. As we would like to understand the dynamics of x at time scales comparable to t_{MRDT} , we consider the case $B(f) \sim B$ in what follows. In this, the stochastic process $\delta F(t)$ in the r.h.s. of Eq. (A2) has correlation properties of white noise:

$$E(\delta F(t)\delta F(t')) = B\delta(t-t'), \quad (\text{A3})$$

where $\delta(t-t')$ is the Dirac delta-function.

3. In the vicinity of a stationary point (homeostasis)

When the genotoxic forces are relatively weak, $|\delta F| \ll [F_0]$, the fluctuations of the expressome state vector are also small: $x = x_0 + \delta x$, $\delta x \ll x_0$. Here x_0 is the stationary point given by the solution of the equation

$$g(x_0) = F_0.$$

In the vicinity of this point Eq. (A2) reduces to

$$D\delta\dot{x} + K\delta x + \Gamma^{(3)}\delta x\delta x + \dots = \delta F, \quad (\text{A4})$$

where the matrices D and K describe the relaxation effects and the "interaction" between genes in the GRN. The matrix $\Gamma^{(3)}$ encodes the leading non-linear terms in the expansion of the vector function $g(x)$ in powers of small δx , while \dots denote higher order terms in this expansion. Generally, such non-linear terms are not small[65] However, a common feature of the dissipative network described by Eq. (A4) is the decay of (most) principal components of δx with time, which makes nonlinearities in Eq. (A4) less relevant at later stages of the time dynamics. Whether this feature holds for the GRN under consideration is a non-trivial question, which we shall now address.

4. Saddle-node bifurcation and critical slowing-down

Domination of a single principle component in the expressome vector $x(t)$ is *not* a generic prediction of the model (A4). We would like to argue that such a dominance implies that GRNs under consideration are operating at the critical point. This critical point is a bifurcation, separating regimes of stable and unstable run-away behavior of the expressome δx .

Transition from stability to instability in networks with network graphs not possessing specific symmetries is typically associated with existence of co-dimension 1 bifurcations [25, 26]. Such transition is characterized by the loss of stability along a single principal component of the network state vector. Contributions from all other principal components remain stable. This situation is known in the literature as saddle-node bifurcation [25] and is realized, when the lowest (real) eigenvalue of the matrix K reaches zero and then becomes negative.

Let us denote the smallest (vanishing, but positive) eigenvalue of the matrix K as ϵ and its corresponding left and right eigenvectors - as a and b . In order to understand dynamics of the expressome δx near the GRN bifurcation, it is convenient to analyze the autocorrelation function $E(\delta x(t)\delta x(t'))$. The latter is given by the following expression (in the frequency domain)

$$\begin{aligned} E(\delta x(t)\delta x^T(t')) &= \\ &= \int df \cdot e^{-2\pi if(t-t')} A^{-1}(f)E(\delta F(-f)\delta F^T(f))A^{*-1}(f), \end{aligned} \quad (\text{A5})$$

where $A(f) = i2\pi Df + K$. Its behavior is determined by the poles of the integrand in the complex plane of frequency f . In turn, the latter are given by the solution of the equation

$$\det(A(f)) = 0,$$

i.e., by the solution of the eigenvalue problem for the matrix $\pm i(2\pi)^{-1}D^{-1}K$. In particular, at very large time separations $|t-t'|$ one finds that

$$E(\delta x(t)\delta x^T(t')) \approx \frac{(a^T \cdot Ba)b \cdot b^T}{\epsilon(a^T \cdot Db)^3} \exp\left(-\frac{\epsilon|t-t'|}{(a^T \cdot Db)}\right). \quad (\text{A6})$$

Several important observations can be made at this point: (1) as the parameter ϵ approaches 0, amplitude of the autocorrelation function (A6) grows as ϵ^{-1} , i.e., fluctuations of the expressome vector are strongly amplified both with age and among the population (the statistical ensemble); (2) the autocorrelation time scale $\tau = (a^T \cdot Db)/\epsilon$ also grows strongly at $\epsilon \rightarrow 0$, implying that stochastic dynamics of the expressome becomes very slow near the point of bifurcation, phenomenon known as critical slowing-down (see for example [27]); (3) fluctuations of the expressome vector δx mostly develop along the direction b of the

right eigenvector of K corresponding to the vanishing eigenvalue ϵ , this in turn guarantees that a single principal component of the expressome vector δx dominates; (4) the corresponding left eigenvector a determines directions of high sensitivity of the expressome to genotoxic stress factors δF .

As the behavior (A6) of the autocorrelation function is dominated by the lowest eigenvalue of the matrix $-i(2\pi)^{-1}D^{-1}K$ (proportional in turn to the lowest eigenvalue ϵ of the matrix K), other remaining eigenvalues of $-i(2\pi)^{-1}D^{-1}K$ have strictly positive real parts and thus correspond to contributions to (A6), rapidly decaying with time. This guarantees that only one principal component of δx dominates, in accordance with experimental observations.[66]

When ϵ crosses 0 and becomes negative, the autocorrelation function (A6) develops unstable behavior, again directed along the corresponding right eigenvector b of K . In particular, one finds for the dispersion of the expressome at large t

$$E(\delta x(t)\delta x^T(t)) \approx E(z^2(0))b \cdot b^T \exp\left(\frac{2\epsilon t}{(a^T \cdot Db)}\right), \quad (\text{A7})$$

where $E(z^2(0))$ is the dispersion of the projection $z = (\delta x^T \cdot b)$ of the expressome on the vector b , taken at the initial moment of time. Dynamics of the expressome δx along other principal components remains stable.

Thus, the quantity of interest in the critical regime $\epsilon \rightarrow 0$ is the projection of the expressome δx on the right eigenvector b :

$$z = (\delta x^T \cdot b),$$

which satisfies the Langevin equation

$$\frac{dz}{dt} = \alpha z + \beta z^2 + \dots + f, \quad E(f(t)f(t')) = \Delta \delta(t-t') \quad (\text{A8})$$

where $\alpha = \epsilon/(a^T \cdot Db)$, $\beta = (a^T \cdot \Gamma^{(3)}bb)/(a^T \cdot Db)$, \dots and $\Delta = (a^T \cdot Ba)/(a^T \cdot Db)^3$.

This concludes the derivation of Eq. (2).

Appendix B: Estimating mortality rates from the stochastic dynamics of expressome

So far we have only considered stochastic dynamics of the expressome state vector δx of an organism. To proceed with population properties, such as mortality, we need to construct a statistical description for populations, ensembles of organisms. Consider a large population of animals with the number of species $N(t=0) = N_0 \gg 1$, born at the same moment of time, $t=0$. The development and ageing of animals in the population depends on the dynamics of the expression levels x and can be naturally described in terms of the probability density $dN = P(x,t) dx$, where $P(x,t)$ is the fraction of of specimen within the population with the gene expression levels within the interval $(x-dx, x+dx)$ estimated at time

t . Another quantity of interest is the survival probability $S(t)$, defined as the ratio of the number of species $N(t)$ still alive at time t to their initial number N_0 . The associated mortality rate can then be found using the expression $M(t) = -\frac{dS}{dt}/S$. In this Section we shall explain how to estimate both the probability density $P(z,t)$, the survival probability $S(t)$ and the mortality rate $M(t)$ from the stochastic dynamics of the expressome state vector δx .

1. Estimating the probability density $P(z,t)$

As was discussed above, the process of ageing is characterized by slow changes in gene expression levels δx over time, described by the Langevin equation (A8). Hereinafter in this Section for the sake of brevity we drop δ in δz , denoting the fluctuation of the expressome δz simply as z . The probability $P(z,t)$ is the solution of the associated Fokker-Planck equation [67]

$$\begin{aligned} \frac{\partial P(z,t)}{\partial t} = & \frac{\partial}{\partial z} ((\alpha z + \beta z^2 + \gamma z^3 + \dots)P(z,t)) + \\ & + \frac{1}{2}\Delta \frac{\partial^2 P(z,t)}{\partial z^2}, \end{aligned} \quad (\text{B1})$$

subject to the initial condition $P(z,t=0) = P_0(z)$ and a boundary condition at large z . In what follows we consider two particular cases: a ‘‘deterministic’’ initial condition

$$P(z,t=0) = \delta(z), \quad (\text{B2})$$

where z is the Dirac delta-function, and the Gaussian initial condition

$$P(z,t=0) = \frac{1}{\sqrt{2\pi\delta z_0^2}} e^{-\frac{(z-z_0)^2}{2\delta z_0^2}}. \quad (\text{B3})$$

A physically relevant choice of the boundary condition at large z is

$$P(z \rightarrow \infty, t) = 0, \quad (\text{B4})$$

implying that all specimen with sufficiently large z associated with high toxicity will necessarily die and drop out from the distribution. Our reasoning behind the choice of this particular boundary condition is as follows. Let us assume that for every gene in the genome there exists a particular threshold X_i of its expression, which is associated with a strong build-up of toxicity in associated pathways and a subsequent inevitable death of a specimen.[68] After the projection on the leading principal component $\sim b$ of the expressome δx most information about the geometry of this ‘‘threshold surface’’ is of course lost. However, one notes that the characteristic time for the stochastic process $z(t)$ to reach infinity $z = \infty$ is *always finite*, as long as non-linear terms

are present in the Fokker-Planck equation (B1), and the state $z = \infty$ is *certainly associated* with the death of the specimen. Thus, expressions for the average lifespan and the survival probability derived below are *at least good upper bounds* on the real average lifespan and survival probability of the species in question.

The choice of the boundary condition (B4) is especially suitable in the case, when non-linearities in Eq. (A8) are taken into account, i.e., at least some of β, γ, \dots in Eq. (B1) are non-zero.

In the case, when only $\alpha \neq 0$ the appropriate counterpart of the boundary condition (B4) is

$$P(z = Z, t) = 0, \quad (\text{B5})$$

meaning that specimen die, when z reaches a certain threshold value Z . The boundary conditions (B4) and (B5) are associated in the following sense. If $\beta \neq 0$, while all other non-linearities in Eq. (A8) are absent, all the expressions for the probability distribution functions and correlation functions of the expressome remain the same as in the linear case, but with a substitution $Z \sim (\alpha/\beta)^{1/2}$. A similar conclusion (but with a slightly different expression for Z) holds, when the next order non-linearity γ is taken into account, see below. Thus, the cases (B4) and (B5) are essentially physically equivalent, and one can switch between the discussion of non-linear Fokker-Planck equation (B1) and the linear one, whenever convenient.

The Fokker-Planck equation (B1) with the boundary conditions (B4) or (B5) cannot be solved exactly. However, this is not really needed: a large amount of useful information about stochastic dynamics of the expressome can be extracted from the asymptotic behavior of the probability density $P(z, t)$ in various physically interesting regimes [27, 69].

In particular, at sufficiently early times $t \ll \alpha^{-1}$ behavior of δz described by the Langevin equation (A8) is entirely dominated by the effect of the random force $f(t)$, dominating over the “deterministic” force $-\alpha z$ [27, 69]. One immediately finds for the case of Gaussian initial distribution (B3):

$$P(z, t) \approx \frac{1}{\sqrt{2\pi E(\delta z^2(t))}} e^{-\frac{(z - E(z(t)))^2}{2E(\delta z^2(t))}}, \quad (\text{B6})$$

where $E(z(t)) = z_0 \exp(\alpha t)$ and

$$E(\delta z^2(t)) = \delta z_0^2 + \left(\delta z_0^2 + \frac{\Delta}{\alpha} \right) (\exp(2\alpha t) - 1). \quad (\text{B7})$$

Therefore, in the average both expressome and its fluctuations grow exponentially with time. This conclusion is confirmed by the data analysis of senescence-associated transcriptional dynamics. It is worth emphasizing that the characteristic time scale of the stochastic growth of the expressome is $\sim \alpha^{-1}$. It thus depends only on the morphological properties of the GRN and does not depend on the genotoxic stress amplitude Δ at all.

The “intermediate” regime realized at $\alpha^{-1} < t \lesssim \alpha^{-1} \log \left(\frac{\alpha^{1/2} Z}{\Delta^{1/2}} \right)$, when the deterministic force αz dominates over the random force $f(t)$ in the Langevin equation (A8), is characterized by so called Suzuki scaling [27, 69]. In this regime, the Fokker-Planck equation (B1) effectively reduces to a deterministic drift equation

$$\frac{\partial P(z, t)}{\partial t} = \frac{\partial}{\partial z} ((\alpha z + \beta z^2 + \gamma z^3 + \dots) P(z, t)).$$

Its solution is

$$P(z, \tau) = \frac{h'(z)}{(2\pi\tau)^{1/2}} \exp\left(-\frac{h^2(z)}{2\tau}\right), \quad (\text{B8})$$

where $\tau = \exp(2\alpha t)$ is the Suzuki time variable, and the function $h(z)$ has to be found on the case-by-case basis by matching the solution (B8) to the solution of the Fokker-Planck equation at early times (for example, to Eq. (B6)). We would like to again emphasize that the expression (B8) holds for both linear and non-linear cases, although the form of the function $h(z)$ will be different for them. The regime of Suzuki scaling will be discussed in more details in the next Subsection.

Finally, no general statement can be made regarding the behavior of $P(z, t)$ at large $t \gg \alpha^{-1} \log \left(\frac{\alpha^{1/2} Z}{\Delta^{1/2}} \right)$. If the function $V(z) = -\int^z dz' (\alpha z' + \beta z'^2 + \gamma z'^3 + \dots)$ has not only a maximum at $z = 0$, but also a true minimum at some large $z = z_{\text{equilib}}$, the probability density $P(z, t)$ approaches a normalizable time-independent asymptotics

$$P(z) \sim \exp\left(-\frac{V''(z_{\text{equilib}})(z - z_{\text{equilib}})^2}{\Delta}\right).$$

On the other hand, if no true minima of the function $V(z)$ exist, the non-normalizable probability density $P(z, t)$ exponentially quickly vanishes at $t \rightarrow +\infty$ (also see below). This choice seems to be a physically appropriate one, since at very high (toxic) values z GRNs simply dissociate, and the whole description of the system state in terms of the leading principal component of δz no longer makes sense.

2. Estimating the first passage time and survival probabilities

In the case under consideration, a more relevant quantity to calculate and analyze is not the probability density $P(z, t)$ itself, but a so called first passage time distribution function $P_{\text{FPT}}(t)$ [70, 71]. The reason is that the probability density $P(z, t)$ represents a sum over all possible stochastic trajectories $z(t)$, including those, which pass the threshold $z = Z$ and then return back. On the other hand, by definition, $P_{\text{FPT}}(T)$ is a probability for a given stochastic trajectory $z = z(t)$ to pass the threshold $z = Z$ at $t = T$ for the very first time. As such, it does not take into account trajectories, which then return back into the allowed domain of z .

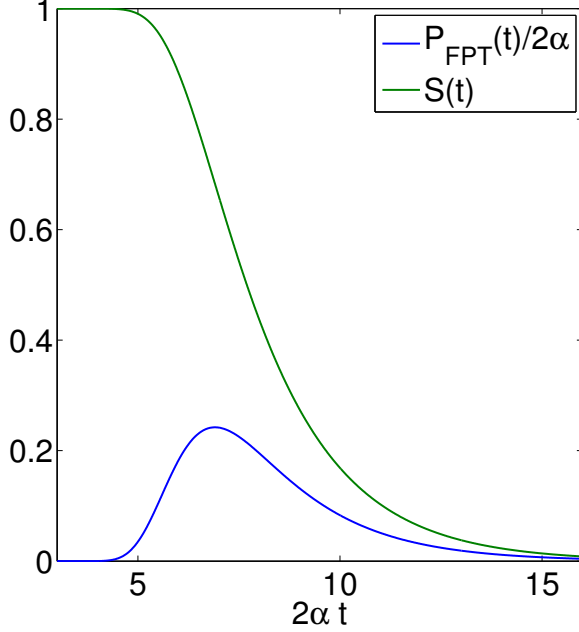


Figure 5: The first passage time distribution function $P_{\text{FPT}}(t)$ (in units of 2α) and the survival probability $S(t)$ as a function of time $2\alpha t$; $\frac{\alpha Z^2}{\Delta} = 1000$.

When a deterministic initial condition (B2) is chosen, the first passage time distribution function is given by

$$P_{\text{FPT}}(t) \approx \frac{2\alpha Z \cdot e^{2\alpha t}}{(e^{2\alpha t} - 1)^{3/2}} \left(\frac{\alpha}{2\pi\Delta}\right)^{1/2} \exp\left(-\frac{\alpha Z^2}{2\Delta(e^{2\alpha t} - 1)}\right), \quad (\text{B9})$$

while for the Gaussian initial condition (B3) one finds

$$P_{\text{FPT}}(t) \approx \frac{2Z\Delta \cdot e^{2\alpha t}}{\sqrt{2\pi} (\delta z_0^2 + (\delta z_0^2 + \frac{\Delta}{\alpha})(e^{2\alpha t} - 1))^{3/2}} \times \exp\left(-\frac{Z^2}{2(\delta z_0^2 + (\delta z_0^2 + \frac{\Delta}{\alpha})(e^{2\alpha t} - 1))}\right). \quad (\text{B10})$$

In the regime of Suzuki scaling $\alpha^{-1} < t \lesssim \alpha^{-1} \log\left(\frac{\alpha^{1/2} Z}{\Delta^{1/2}}\right)$ the expression (B9) reduces to

$$P_{\text{FPT}}(t) \approx 2\alpha Z \left(\frac{\alpha}{2\pi\Delta}\right)^{1/2} \exp\left(-\alpha t - \frac{\alpha Z^2}{2\Delta} e^{-2\alpha t}\right), \quad (\text{B11})$$

well known in literature. The function (B11) grows exponentially at small $t \lesssim \alpha^{-1}$, possesses a distinct maximum at $t_{\text{max}} = E(t_{\text{ls}}) = \alpha^{-1} \log\left(\left(\frac{\alpha Z^2}{\Delta}\right)^{1/2}\right)$, with its width $\delta t \sim \alpha^{-1}$ near the maximum and finally decays as $e^{-\alpha t}$ at $t \gg t_{\text{max}}$, see Fig. 5.

Computing the first passage time distribution function also allows one to easily estimate the survival probability

$S(t)$, using the prescription $P_{\text{FPT}}(t) = -\frac{dS(t)}{dt}$. From Eq. (B11) we immediately find

$$S(t) \approx \text{Erf}\left(\left(\frac{\alpha Z^2}{2\Delta}\right)^{1/2} e^{-\alpha t}\right), \quad (\text{B12})$$

expression precise up to terms, exponentially small at $\frac{\alpha Z^2}{\Delta} \gg 1$, i.e., when a species is considered long-lived compared to the characteristic time scales of molecular dynamics in the cell, see the next Subsection. The function (B12), initially exponentially close to 1, then falls off quickly (as we shall see below, this fall-off corresponds to an exponentially growing mortality rate) and finally approaches zero as $\exp(-\alpha t)$ at $t \gg \alpha^{-1} \log\left(\frac{\alpha^{1/2} Z}{\Delta^{1/2}}\right)$.

3. Average lifespan

Although it is impossible to find an exact solution for the first passage time distribution function and the survival probability in a generic non-linear case with $\beta, \gamma, \dots \neq 0$ (expressions found in the previous Subsection are only generally valid in the regime of Suzuki scaling), it is possible to find a closed form expression for the average lifespan $E(t_{\text{ls}})$ within the population as well as arbitrarily high moments $E(t_{\text{ls}}^n)$ of the lifespan. Here we shall present the final result for $E(t_{\text{ls}})$ without derivation:

$$E(t_{\text{ls}}) = \frac{1}{\Delta} \int_{z_0}^{+\infty} dz \cdot \exp(-2v(z)) \int_z^{+\infty} dz' \exp(2v(z')),$$

where $v(z) = \frac{V(z)}{\Delta} = -\frac{1}{\Delta} \left(\frac{1}{2}\alpha z^2 + \frac{1}{3}\beta z^3 + \dots\right)$. In particular, for the case $\alpha, \beta \neq 0, \gamma = 0, \dots$ one immediately finds

$$E(t_{\text{ls}}) \approx \frac{1}{\alpha} \log\left(\frac{\alpha}{\beta^{1/2} \Delta^{1/2}}\right) \quad (\text{B13})$$

at large $\frac{\alpha}{\beta^{1/2} \Delta^{1/2}} \gg 1$. Similarly, in the case $\alpha \neq 0, \beta = 0, \gamma \neq 0, \dots$ one finds

$$E(t_{\text{ls}}) \approx \frac{1}{\alpha} \log\left(\frac{\alpha^2}{\gamma \Delta^2}\right),$$

etc. One again sees that non-linear cases are equal to the linear one with the appropriately chosen threshold value Z (for instance, $Z = (\alpha/\beta)^{1/2}$ in the case $\beta \neq 0, Z_{\text{eff}} = \alpha^{3/2}/(\gamma \Delta^{3/2})$ in the case $\beta = 0, \gamma \neq 0$, etc.).

It is interesting to note that the average lifespan depends strongly on the morphological properties (topology, connectivity) of the GRN through the dependence on α^{-1} , while the characteristic amount of stress (its amplitude given by Δ) affects the value of $E(t_{\text{ls}})$ only logarithmically weakly.

4. Behavior of the mortality rate

As usual, the mortality rate is defined following the prescription $M(t) = -\frac{dS}{dt}/S$, so that one has precisely

$$M(t) = \frac{P_{\text{FPT}}(t)}{S(t)}. \quad (\text{B14})$$

We shall now focus on the particular case of the deterministic initial condition (B2).

a. Vanishing mortality at very early ages $t \ll \alpha^{-1}$

At very early ages $t \ll \alpha^{-1}$ the first passage time distribution function is exponentially strongly suppressed:

$$P_{\text{FPT}}(t) \approx \frac{2\alpha Z}{(2\alpha t)^{3/2}} \left(\frac{\alpha}{2\pi\Delta}\right)^{1/2} \exp\left(-\frac{Z^2}{4\Delta t}\right). \quad (\text{B15})$$

In this regime the survival probability $S(t)$ remains exponentially close to 1:

$$S(t) \approx 1 - \frac{2}{\sqrt{\pi}} \left(\frac{4\Delta t}{Z^2}\right)^{1/2} \exp\left(-\frac{Z^2}{4\Delta t}\right).$$

Therefore, the mortality rate remains exponentially close to 0, and one approximately has $M(t) \approx P_{\text{FPT}}(t)$. From our opinion, this behavior might explain relatively small mortality, often observed in cohorts at very early ages. We note that the behavior of the mortality rate in this regime is not universal as it strongly depends on the amplitude Δ of stochastic genotoxic stress.

b. Gompertz behavior at later ages $0.54\alpha^{-1} < t \lesssim \alpha^{-1}$

As was explained above, the effect of the stochastic force δF in Eq. (A4) quickly becomes negligible with age in comparison to the effect of the ‘‘deterministic’’ force $-K\delta x$; one can easily find from the expression (B7) that the two effects become comparable at times $t_0 \approx \alpha^{-1} \log(\sqrt{3}) \approx 0.54\alpha^{-1}$, and the ‘‘deterministic’’ force then always dominates at later times $t > t_0$ [27, 69]. Correspondingly, the behavior (B15) quickly changes at later times $t_0 < t \lesssim \alpha^{-1}$, leading to the Gompertz-like dependence of the mortality rate on age. For the mean square deviation $E(\delta z^2)$ one finds $E(\delta z^2(t_0)) = \delta z_0^2 \approx \frac{\Delta}{\alpha} (\exp(2\alpha t_0) - 1)$ at the time t_0 , and thus $E(\delta z^2(t)) \approx \delta z_0^2 + 2(\delta z_0^2 + \Delta/\alpha) (e^{2\alpha(t-t_0)} - 1)$ at later times $t_0 < t \lesssim \alpha^{-1}$. As the survival probability is still very close to 1, and the mortality rate is completely determined by the behavior of the first passage time distribution function, one finds the following expression for the logarithm of the mortality rate

$$\log M(t) \approx -\frac{Z^2}{4\Delta t_0} + \log 2Z\Delta + 2\alpha t_0 + \left(\frac{Z^2(2\alpha t_0 + 1)}{2t_0} + 2\alpha\right) \left(\frac{t-t_0}{t_0}\right). \quad (\text{B16})$$

The value of the Gompertz exponent is thus equal to

$$\frac{Z^2(2\alpha t_0 + 1)}{2t_0} + 2\alpha \approx \frac{Z^2}{2t_0} \approx \alpha Z^2 = \frac{\alpha^2}{\beta}.$$

This expression is manifestly universal, as it depends on morphological properties of the GRN only through the parameters α and β characterizing GRN.

c. Universal Gompertz behavior in the regime of Suzuki scaling

At even later times of the order $t \sim E(t_{\text{ls}})$, when the regime of Suzuki scaling is realized, we also find a universal Gompertz behavior. As was explained above, the first passage time probability distribution P_{FPT} reaches a maximum at $t_{\text{max}} = \alpha^{-1} \log \Lambda = E(t_{\text{ls}})$, where $\Lambda = \frac{\alpha^{1/2} Z}{\Delta^{1/2}}$, and its half-width near the the maximum is of the order α^{-1} , see Fig. 5. By the time $t \sim t_{\text{max}}$ the argument of the error function in Eq. (B12) is already sufficiently small for it to be expanded. One thus has

$$S(t) \approx \frac{2}{\sqrt{\pi}} \Lambda e^{-\alpha t} - \frac{2}{3\sqrt{\pi}} \Lambda^3 \exp(-3\alpha t) + \dots$$

One the other hand, one finds for $P_{\text{FPT}}(t)$ in the same regime

$$P_{\text{FPT}}(t) = \frac{2\alpha\Lambda}{\sqrt{\pi}} e^{-\Lambda^2 \exp(-2\alpha t)} e^{-\alpha t},$$

so that approximately

$$M(t) \approx \alpha e^{-\Lambda^2 \exp(-2\alpha t)}.$$

Introducing $t = t_{\text{max}} + \delta t$ one finally finds at small $\delta t \lesssim (2\alpha)^{-1}$

$$M(t) \approx e^{-1/2} \alpha e^{\alpha \delta t} \approx 0.61 \alpha e^{\alpha \delta t}. \quad (\text{B17})$$

Thus, the Gompertz law with the universal exponent α^{-1} is realized at times $t_{\text{max}} - (2\alpha)^{-1} \lesssim t \lesssim t_{\text{max}} + (2\alpha)^{-1}$. We again emphasize that the Gompertz rate depends only on the properties of the GRN under consideration and does not depend on stress. The transition between the regimes (B16) and (B17) is smooth.

d. Slowing-down of mortality at late ages

Finally, at $t \gg t_{\text{max}}$ both the first passage time distribution function (B11) and the survival probability (B12) decay exponentially. This corresponds to an asymptotically constant behavior of the mortality rate

$$M(t) \approx \alpha - \frac{\alpha^2 Z^2}{2\Delta} e^{-2\alpha t} - \dots, \quad (\text{B18})$$

see Fig. 6. For late t corrections to the leading constant term become exponentially small with time. The existence of mortality plateau in models of the type (A4) is known in literature [72, 73].

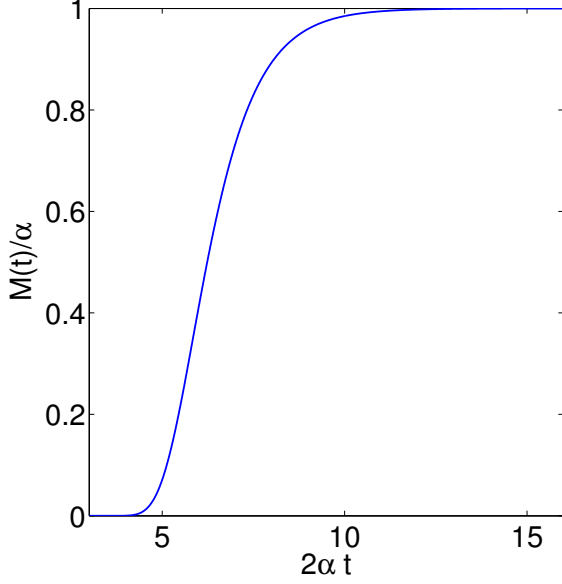


Figure 6: The mortality rate $M(t)$ for the case of the deterministic initial conditions (B2); $\frac{\alpha Z^2}{\Delta} = 1000$. The maximum of $P_{\text{FPT}}(t)$ is reached at $2\alpha t \approx 6.9$.

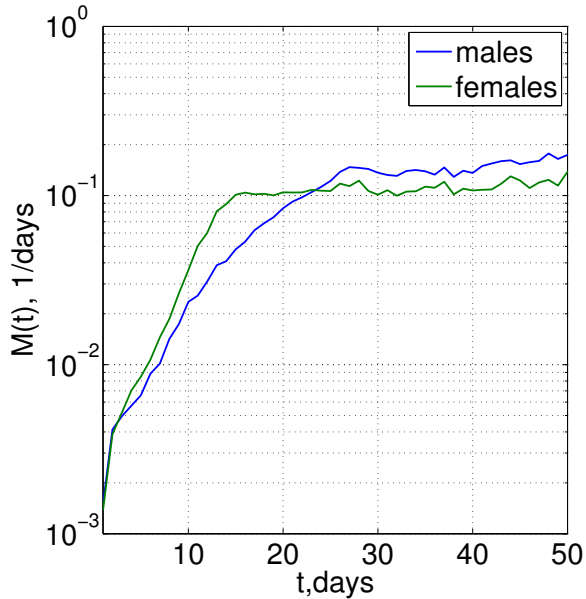


Figure 7: The mortality rate as a function of age from the very large cohorts study, medflies, males and females from [21].

5. Phenomenology of the different regimes of ageing

a. The case $\frac{\alpha Z^2}{\Delta} \gg 1$

This case includes the one with a very weak non-linearity in the Fokker-Planck equation (B1) and $Z^2 \sim \alpha/\beta$ and corresponds to a very high toxicity threshold Z as compared to the characteristic amplitude of fluctuations of the stress factors Δ . As was explained above, we naively expect a species with such a GRN to be relatively long-lived, as the average life expectancy (B13) is logarithmically larger than the inverse Gompertz exponent α^{-1} . Four very distinct regimes of mortality exist for such species: (a) the regime of small mortality at early ages, (b) a Gompertz regime with the Gompertz exponent $\sim \frac{\alpha^2}{\beta} \gg \alpha$, (b) a Gompertz regime with a universal Gompertz exponent α and finally (c) a regime of constant mortality $M_\infty \sim \alpha$. On the other hand, if indeed $Z \gg \sqrt{\delta z_0^2}$, the initial Gompertz exponent is very large, and an arbitrary not too strongly sized population simply dies out before the regime of mortality slowing-down is observed. The observed value of the average lifespan in such populations is lower than the estimate (B13). However, it strongly depends on the size of the population; increasing this size would lead to an apparent extension of the observed average lifespan and eventually — to the observation of the regime of mortality slowing-down. This is perhaps what we observe in very large cohorts of *Homo sapiens*. Note that (a) the observed value of the Gompertz exponent $\sim \alpha^2/\beta$ is much larger than the mortality M_∞ at late ages, (b) the value of the Gompertz exponent is relatively insensitive to the amplitude Δ of genotoxic stress, since it only depends on the morphological properties of the GRN of a species.

b. The case $\frac{\alpha Z^2}{\Delta} \gtrsim 1$

There are again four distinct regimes (a), (b), (c) and (d) of ageing discussed above, with that difference that the regime (b) is a Gompertz regime with the exponent $\sim \alpha$. Clearly, the regimes (b) and (c) are very close to each other, and there is a strong correlation between the observed value of the Gompertz exponent and the mortality rate M_∞ at late ages. This, as it seems, is what we observe in *D. melanogaster*, see Fig. 2A&C of the main text of the paper. A relatively short average lifespan of such species is comparable to the value of Gompertz exponent.

c. The case $\alpha < 0, \beta > 0$

In this case, arguably the most tempting to consider, the effective potential $V(z)$ of the Langevin equation possesses a false minimum, separated from the roll-down to

$z \rightarrow \infty$ by a potential barrier, see Fig. 1d of the main text. There exists a single regime of ageing realized for the GRN of this type. It is characterized by a constant mortality rate M_∞ , its value being determined by the exponentially small Kramers probability of passage through

the barrier. If a GRN with such properties indeed exists in nature, it would correspond to a species with negligible senescence. We leave the in-depth study of this regime for a future work.

-
- [1] Partridge, L. & Gems, D. Mechanisms of ageing: public or private? *Nat. Rev. Genet.* **3**, 165–75 (2002). URL <http://dx.doi.org/10.1038/nrg753>.
- [2] Sinclair, D. A. & Oberdoerffer, P. The ageing epigenome: damaged beyond repair? *Ageing Res. Rev.* **8**, 189–98 (2009). URL <http://www.sciencedirect.com/science/article/pii/S1568163709000245>.
- [3] Gladyshev, V. N. On the cause of aging and control of lifespan: heterogeneity leads to inevitable damage accumulation, causing aging; control of damage composition and rate of accumulation define lifespan. *Bioessays* **34**, 925–9 (2012).
- [4] Gladyshev, V. N. The origin of aging: imperfectness-driven non-random damage defines the aging process and control of lifespan. *Trends Genet.* **29**, 506–12 (2013).
- [5] Blagosklonny, M. V. Aging and immortality: quasi-programmed senescence and its pharmacologic inhibition. *Cell Cycle* **5**, 2087–2102 (2006).
- [6] Blagosklonny, M. V. & Hall, M. N. Growth and aging: a common molecular mechanism. *Ageing* **1**, 357 (2009).
- [7] Kirkwood, T. B. L. Evolution of ageing. *Nature* **270**, 301–304 (1977).
- [8] Kirkwood, T. B. & Austad, S. N. Why do we age? *Nature* **408**, 233–8 (2000).
- [9] Williams, G. Pleiotropy, natural selection, and the evolution of senescence. *Science's SAGE KE* **2001**, 13 (2001).
- [10] Reis, R. J. S. Model systems for aging research: syncretic concepts and diversity of mechanisms. *Genome* **31**, 406–412 (1989).
- [11] Skulachev, V. The programmed death phenomena, aging, and the Samurai law of biology. *Exp. Gerontol.* **36**, 995–1024 (2001).
- [12] Longo, V. D., Mitteldorf, J. & Skulachev, V. P. Programmed and altruistic ageing. *Nat. Rev. Genet.* **6**, 866–72 (2005).
- [13] de Magalhães, J. a. P. Programmatic features of aging originating in development: aging mechanisms beyond molecular damage? *FASEB J.* **26**, 4821–6 (2012). URL <http://www.fasebj.org/content/26/12/4821.short>.
- [14] Orgel, L. E. Ageing of Clones of Mammalian Cells. *Nature* **243**, 441–445 (1973).
- [15] Hopfield, J. J. Kinetic Proofreading: A New Mechanism for Reducing Errors in Biosynthetic Processes Requiring High Specificity. *Proc. Natl. Acad. Sci.* **71**, 4135–4139 (1974).
- [16] Danchin, A. Natural selection and immortality. *Biogerontology* **10**, 503–16 (2009).
- [17] Kogan, V., Molodtsov, I., Menshikov, L. I., Reis, R. J. S. & Fedichev, P. Stability analysis of a model gene network links aging, stress resistance, and negligible senescence. *arXiv preprint arXiv:1408.0463* (2014).
- [18] Antoulas, A. C. *Approximation of Large-Scale Dynamical Systems* (SIAM, 2009).
- [19] Pletcher, S. D. *et al.* Genome-wide transcript profiles in aging and calorically restricted *Drosophila melanogaster*. *Current Biology* **12**, 712–723 (2002).
- [20] Avanesov, A. S. *et al.* Age- and diet-associated metabolome remodeling characterizes the aging process driven by damage accumulation. *eLife* **3** (2014).
- [21] Vaupel, J. W. *et al.* Biodemographic trajectories of longevity. *Science* **280**, 855–860 (1998).
- [22] Horvath, S. Dna methylation age of human tissues and cell types. *Genome biology* **14**, R115 (2013).
- [23] Balleza, E. *et al.* Critical dynamics in genetic regulatory networks: examples from four kingdoms. *PLoS One* **3**, e2456 (2008).
- [24] Krotov, D., Dubuis, J. O., Gregor, T. & Bialek, W. Morphogenesis at criticality. *Proceedings of the National Academy of Sciences* **111**, 3683–3688 (2014).
- [25] Fiedler, B. E. *Handbook of Dynamical Systems, Volume 2* (Gulf Professional Publishing, 2002).
- [26] Seydel, R. *Practical Bifurcation and Stability Analysis*, vol. 1 (Springer Science & Business Media, 2009).
- [27] Suzuki, M. Passage from an initial unstable state to a final stable state. In *Advances in Chemical Physics, Volume 46*, 195–276 (John Wiley & Sons, 2009). URL <http://books.google.com/books?hl=en&lr=&id=6uAY7tkKEVkc&pgis=1>.
- [28] The latter observation is supported by the analysis of the recent experiments in *D. melanogaster*, where transcriptional responses to different stress factors were found to contain a good fraction of similar differentially expressed genes both in the limit of nearly lethal [60] and weak stressors [48].
- [29] Morse, C. Does variability increase with age? an archival study of cognitive measures. *Psychol Aging* **8**, 156–64 (1993).
- [30] Rother, P. The aging changes of biological variability (author's transl). *ZFA* **33**, 463–6 (1978).
- [31] Khalyavkin, A. & Krutko, V. Aging is a simple deprivation syndrome driven by a quasi-programmed preventable and reversible drift of control system set points due to inappropriate organism-environment interaction. *Biochemistry (Moscow)* **79**, 1133–1135 (2014).
- [32] Arlia-Ciommo, A., Piano, A., Leonov, A., Svistkova, V. & Titorenko, V. I. Quasi-programmed aging of budding yeast: a trade-off between programmed processes of cell proliferation, differentiation, stress response, survival and death defines yeast lifespan. *Cell Cycle* **13**, 3336–3349 (2014).
- [33] Blagosklonny, M. V. Answering the ultimate question "what is the proximal cause of aging?". *Ageing* **4**, 861–877 (2012).
- [34] Blagosklonny, M. V. Mtor-driven quasi-programmed aging as a disposable soma theory. *Cell Cycle* **12**, 1842–1847 (2013).

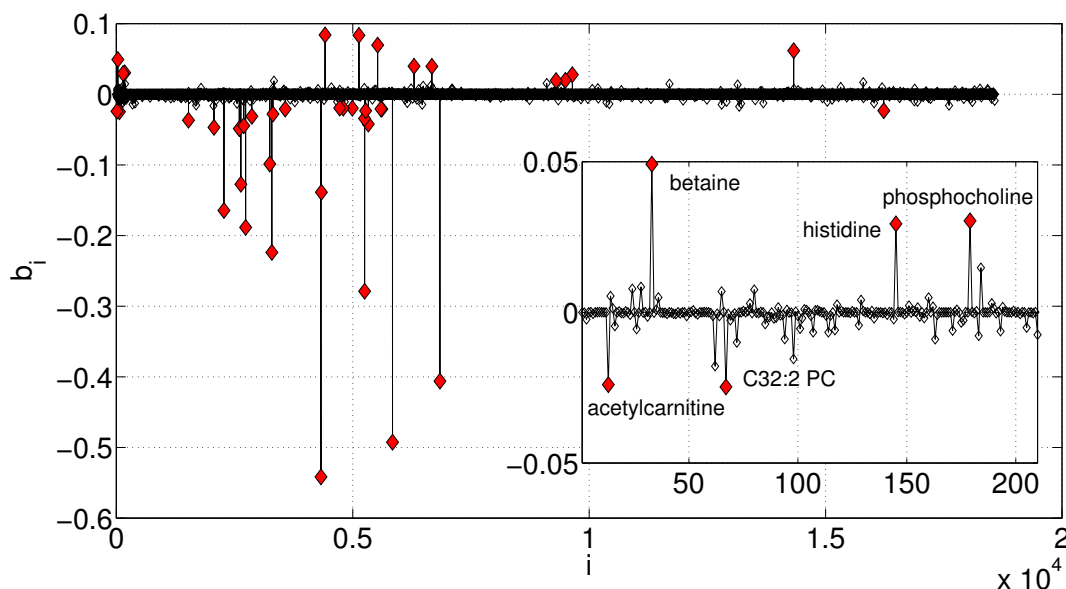


Figure 8: Components of the vector b for *D. melanogaster*, calculated from the full metabolic profiles (including all detected targeted and non-targeted metabolites) from [20].

- [35] Gompertz, B. On the nature of the function expressive of the law of human mortality, and on a new mode of determining the value of life contingencies. *Philosophical transactions of the royal society of London* **115**, 513–583 (1825).
- [36] Gems, D. & Doonan, R. Antioxidant defense and aging in *c. elegans*: is the oxidative damage theory of aging wrong? *Cell Cycle* **8**, 1681–1687 (2009).
- [37] Tacutu, R. *et al.* Human ageing genomic resources: Integrated databases and tools for the biology and genetics of ageing. *Nucleic acids research* **41**, D1027–D1033 (2013).
- [38] Khan, I. & Prasad, N. The aging of the immune response in *drosophila melanogaster*. *The Journals of Gerontology Series A: Biological Sciences and Medical Sciences* **68**, 129–135 (2013).
- [39] Zhou, D. *et al.* Mechanisms underlying hypoxia tolerance in *drosophila melanogaster*: hairy as a metabolic switch. *PLoS genetics* **4**, e1000221 (2008).
- [40] Overschee, V. & Moor, D. *Subspace Identification for Linear Systems: Theory, Implementation, Applications* (Kluwer Academic, 1996).
- [41] Ferguson, M., Mockett, R., Shen, Y., Orr, W. & Sohal, R. Age-associated decline in mitochondrial respiration and electron transport in *drosophila melanogaster*. *Biochem. J* **390**, 501–511 (2005).
- [42] Poynter, M. E. & Daynes, R. A. Peroxisome proliferator-activated receptor α activation modulates cellular redox status, represses nuclear factor- κ b signaling, and reduces inflammatory cytokine production in aging. *Journal of Biological Chemistry* **273**, 32833–32841 (1998).
- [43] Gómez-Valadés, A. G. *et al.* Overcoming diabetes-induced hyperglycemia through inhibition of hepatic phosphoenolpyruvate carboxykinase (gtp) with rnai. *Molecular Therapy* **13**, 401–410 (2006).
- [44] Blagosklonny, M. V. Validation of anti-aging drugs by treating age-related diseases. *Ageing* **1**, 281 (2009).
- [45] Budovskaya, Y. V. *et al.* An *elt-3/elt-5/elt-6* gata transcription circuit guides aging in *c. elegans*. *Cell* **134**, 291–303 (2008).
- [46] Hayflick, L. Entropy explains aging, genetic determinism explains longevity, and undefined terminology explains misunderstanding both. *PLoS Genet.* **3**, e220 (2007).
- [47] Christensen, K., Doblhammer, G., Rau, R. & Vaupel, J. W. Ageing populations: the challenges ahead. *Lancet* **374**, 1196–208 (2009). URL <http://www.sciencedirect.com/science/article/pii/S0140673609614604>.
- [48] Moskalev, A. *et al.* Mining gene expression data for pollutants (dioxin, toluene, formaldehyde) and low dose of gamma-irradiation. *PLoS ONE* **9**, e86051 (2014). URL <http://dx.doi.org/10.1371/journal.pone.0086051>.
- [49] American medical association, resolution 420 (a-13): recognition of obesity as a disease. In *Proceedings of the House of Delegates 162nd Annual Meeting* (2013).
- [50] Ren, C., Webster, P., Finkel, S. E. & Tower, J. Increased internal and external bacterial load during *drosophila* aging without life-span trade-off. *Cell metabolism* **6**, 144–152 (2007).
- [51] Finch, C. E. *Longevity, senescence, and the genome* (University of Chicago Press, 1994).
- [52] Buffenstein, R. The naked mole-rat: a new long-living model for human aging research. *The Journals of Gerontology Series A: Biological Sciences and Medical Sciences* **60**, 1369–1377 (2005).
- [53] Kim, E. B. *et al.* Genome sequencing reveals insights into physiology and longevity of the naked mole rat. *Nature* **479**, 223–227 (2011).
- [54] Jeannette Loram, A. B. Age-related changes in gene expression in tissues of the sea urchin *strongylocentrotus franciscanus*. *Mechanisms of Ageing and Development* **133**, 338–347 (2012).

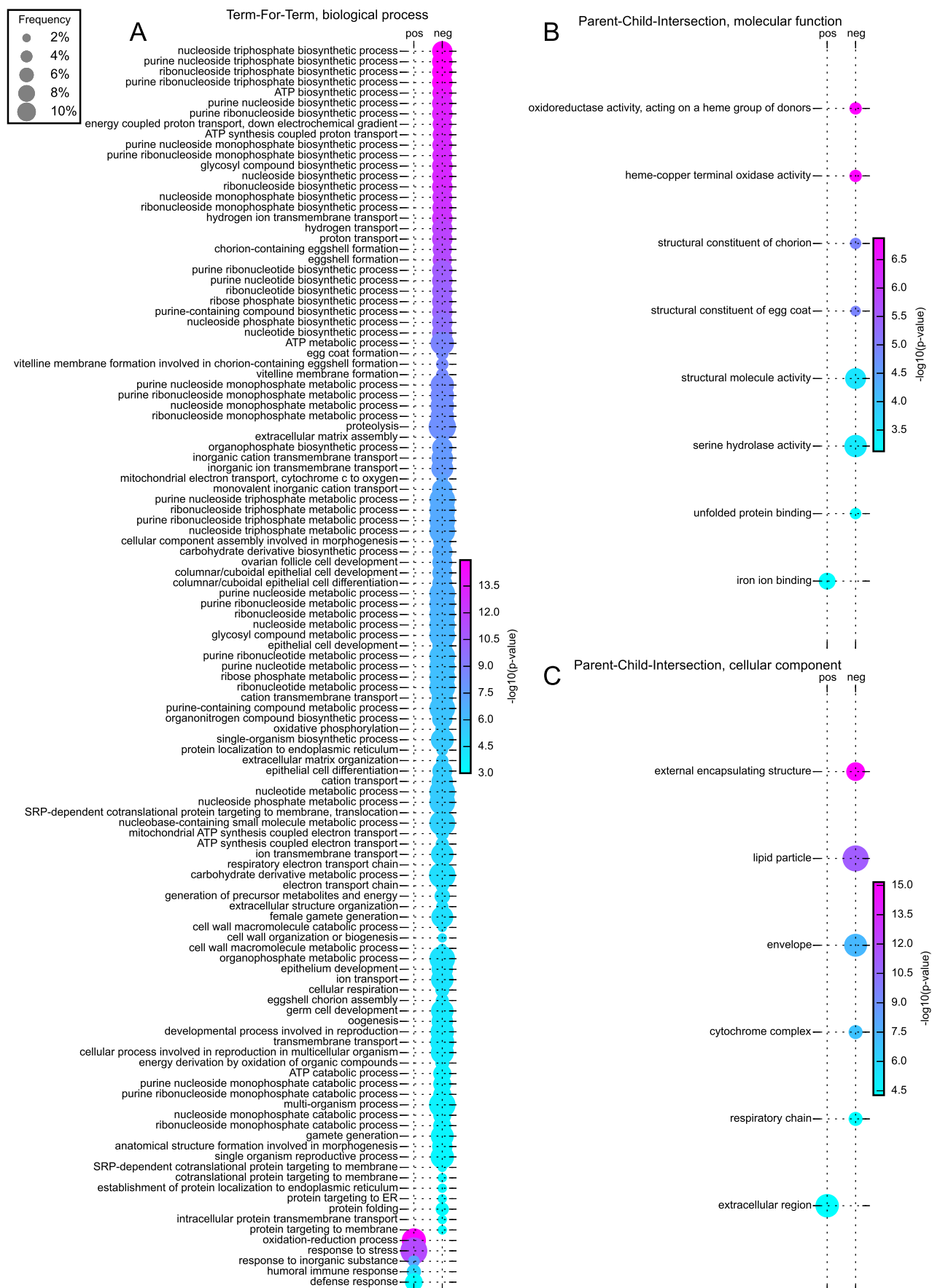


Figure 9: GO enrichment analysis of the leading gene compounds of the ageing direction, *b*. (A) Term-by-term results summary, Biological Process only (cf to Figure 3a); Parent-Child-Intersection results, (B) Cellular Compartment and (C) Molecular Function.

- [55] Bauer, S., Gagneur, J. & Robinson, P. N. Going bayesian: model-based gene set analysis of genome-scale data. *Nucleic acids research* **38**, 3523–3532 (2010).
- [56] Grossmann, S., Bauer, S., Robinson, P. N. & Vingron, M. Improved detection of overrepresentation of gene-ontology annotations with parent–child analysis. *Bioinformatics* **23**, 3024–3031 (2007).
- [57] Da Wei Huang, B. T. S. & Lempicki, R. A. Systematic and integrative analysis of large gene lists using david bioinformatics resources. *Nature protocols* **4**, 44–57 (2008).
- [58] Huang, D. W., Sherman, B. T. & Lempicki, R. A. Bioinformatics enrichment tools: paths toward the comprehensive functional analysis of large gene lists. *Nucleic acids research* **37**, 1–13 (2009).
- [59] Xia, J., Mandal, R., Sinelnikov, I. V., Broadhurst, D. & Wishart, D. S. Metaboanalyst 2.0—a comprehensive server for metabolomic data analysis. *Nucleic acids research* **40**, W127–W133 (2012).
- [60] Brown, J. B. *et al.* Diversity and dynamics of the drosophila transcriptome. *Nature* (2014).
- [61] Kadish, I. *et al.* Hippocampal and cognitive aging across the lifespan: a bioenergetic shift precedes and increased cholesterol trafficking parallels memory impairment. *The Journal of Neuroscience* **29**, 1805–1816 (2009).
- [62] The number of different principal components PC_n representing the signal $x(t_1), \dots, x(t_m)$ does not exceed m .
- [63] Schervish, M. J. *Theory of Statistics*, vol. 21 (Springer New York, 2011).
- [64] In particular, the rate of these changes is limited by a single gene transcription time, ~ 1 min.
- [65] In particular, they are not small at early times, close to the initial state of the expressome.
- [66] When higher order derivatives in Eq. (A1) are taken into account, this argument, albeit becoming more involved, remains valid: one has to construct the perturbation theory in powers of small parameter ϵ , which still determines the smallest eigenvalue of the matrix $A(f) = K + i2\pi fD + (2\pi f)^2M + \dots$. Similarly to the case considered here, all higher eigenvalues of $A(f)$ possess positive real parts.
- [67] Zwanzig, R. *Nonequilibrium Statistical Mechanics* (Oxford University Press, USA, 2001).
- [68] Of course, albeit natural, this is still an assumption, as different gene expressions are not truly independent GRN state variables.
- [69] Suzuki, M. Scaling theory of transient phenomena near the instability point. *Journal of Statistical Physics* **16**, 11–32 (1977). URL <http://link.springer.com/10.1007/BF01014603>.
- [70] Redner, S. *A Guide to First-Passage Processes* (Cambridge University Press, 2001).
- [71] Aalen, O., Borgan, O. & Gjessing, H. *Survival and Event History Analysis: A Process Point of View* (Springer, 2008).
- [72] Weitz, J. S. & Fraser, H. B. Explaining mortality rate plateaus. *Proc. Natl. Acad. Sci. U. S. A.* **98**, 15383–6 (2001).
- [73] Steinsaltz, D. & Evans, S. N. Markov mortality models: implications of quasistationarity and varying initial distributions. *Theor. Popul. Biol.* **65**, 319–37 (2004).

[Competing Interests] The authors declare that they have no competing financial interests.

[Author Contributions] All authors contributed equally to this work.

[Correspondence] Correspondence and requests for materials should be addressed to P.O.F. (email: peter.fedichev@gmail.com) and D.P. (email: dpodolskiy@research.bwh.harvard.edu).